

Phosphorylation of CDC25C by AMP-activated protein kinase mediates a metabolic checkpoint during cell-cycle G₂/M-phase transition

Received for publication, December 11, 2017, and in revised form, February 1, 2018. Published, Papers in Press, February 21, 2018, DOI 10.1074/jbc.RA117.001379

Yuqing Shen^{‡§}, John William Sherman[‡], Xuyong Chen[‡], and Ruoning Wang^{‡1}

From the [‡]Center for Childhood Cancer and Blood Diseases, Hematology/Oncology and BMT, Research Institute at Nationwide Children's Hospital, Ohio State University, Columbus, Ohio 43205 and the [§]Department of Microbiology and Immunology, Key Laboratory of Developmental Genes and Human Disease, Ministry of Education, Medical School, Southeast University, Nanjing 210009, China

Edited by Phyllis I. Hanson

From unicellular to multicellular organisms, cell-cycle progression is tightly coupled to biosynthetic and bioenergetic demands. Accumulating evidence has demonstrated the G₁/S-phase transition as a key checkpoint where cells respond to their metabolic status and commit to replicating the genome. However, the mechanism underlying the coordination of metabolism and the G₂/M-phase transition in mammalian cells remains unclear. Here, we show that the activation of AMP-activated protein kinase (AMPK), a highly conserved cellular energy sensor, significantly delays mitosis entry. The cell-cycle G₂/M-phase transition is controlled by mitotic cyclin-dependent kinase complex (CDC2-cyclin B), which is inactivated by WEE1 family protein kinases and activated by the opposing phosphatase CDC25C. AMPK directly phosphorylates CDC25C on serine 216, a well-conserved inhibitory phosphorylation event, which has been shown to mediate DNA damage-induced G₂-phase arrest. The acute induction of CDC25C or suppression of WEE1 partially restores mitosis entry in the context of AMPK activation. These findings suggest that AMPK-dependent phosphorylation of CDC25C orchestrates a metabolic checkpoint for the cell-cycle G₂/M-phase transition.

Somatic cell-cycle progression involves a doubling and then equal distribution of cellular components and macromolecules into the two daughter cells. As such, interphase (G₁, S, and G₂ phases) represents a long period of cellular growth (accumulation of mass due to anabolic processes), whereas mitosis is the period of division, which is short and accompanied by metabolic suppression (1). Consequently, a fundamental problem in mammalian cells is coordination of the metabolic status with cell-cycle progression (2–6). The progression through the G₁

phase in the mammalian cell cycle is regulated by growth factor/mitogen-mediated signals and metabolic status. The latter remotely resembles a mechanism in yeast known as START and represents a nutrient-sensing metabolic checkpoint (7–11). The signaling network behind the G₁-phase metabolic checkpoint coordinates the cell-cycle machinery and metabolic activities, thus ensuring the availability of energy and nucleotide precursors for genome replication and a timely transition from G₁ to S phase (12–15). Also, it has been suggested that a sufficient storage of energy and biosynthetic materials may enable the execution of mitosis in a robust and all-or-none fashion (16–19). It is conceivable that a cell size-sensing mechanism may play a role in coordinating metabolic status (growth) and the G₂/M-phase transition. This mechanism would allow cells to keep biosynthetic activity in check, ensuring sufficient biomass accumulation to produce daughter cells with the proper size (20–24). These studies implicate the existence of metabolic checkpoints during the G₁/S- and G₂/M-phase transition.

The AMP-activated protein kinase (AMPK)² complex is a central signaling node that keeps the cellular metabolic status in check by sensing changes in cellular AMP and other cellular metabolites, indicative of energy and nutrient status. Upon its activation, AMPK acts to maintain ATP homeostasis by rewiring metabolic programs to produce more energy and meanwhile suppressing many energy-consuming cellular processes, including cell-cycle progression (25, 26). It has been known that AMPK activation inhibits cell proliferation by increasing p21 and p27, two inhibitors of cyclin-dependent kinase (CDK) complex. Under conditions of insufficient nutrients, such as low glucose in cell culture medium, AMPK phosphorylates transcription factor p53, and this phosphorylation event mediates the suppression of G₁-phase progression under glucose restriction (27–30). The mammalian target of rapamycin (mTOR), an

This work was supported by National Institute of Health Grant 1R01AI114581, V-Foundation Grant V2014-001, American Cancer Society Grant 128436-RSG-15-180-01-LIB, and a research grant from the CancerFree KIDs Foundation (to R.W.). The authors declare that they have no conflicts of interest with the contents of this article. The content is solely the responsibility of the authors and does not necessarily represent the official views of the National Institutes of Health.

✂ Author's Choice—Final version free via Creative Commons CC-BY license.

This article contains Tables S1–S3 and Figs. S1–S5.

¹ To whom correspondence should be addressed. Tel.: 614-335-2980; Fax: 614-722-5895; E-mail: ruoning.wang@nationwidechildrens.org.

² The abbreviations used are: AMPK, AMP-activated protein kinase; CDK, cyclin-dependent kinase; mTOR, mammalian target of rapamycin; AICAR, 5-aminoimidazole-4-carboxamide 1-β-D-ribofuranoside; PI, propidium iodide; BrdU, bromodeoxyuridine; PPP, pentose phosphate pathway; ERK, extracellular signal-regulated kinase; ATPγS, adenosine 5'-O-(thiotriphosphate); AS, analog-specific; thioP, thiophosphate; 2DG, 2-deoxyglucose; LKB1, liver kinase B1; DMEM, Dulbecco's modified Eagle's medium; GST, glutathione S-transferase; MBP, maltose-binding protein.

AMPK phosphorylates CDC25C and regulates mitosis entry

evolutionarily conserved protein kinase, integrates environmental cues to coordinately regulate many fundamental cellular processes, including cell-cycle progression through the G₁ phase. AMPK has been reported to directly phosphorylate key components of mTORC1 and consequently suppress mTORC1 signaling and the G₁/S-phase transition (31–36). These findings clearly implicate AMPK as a key player in coupling the cellular metabolic status to the regulation of the G₁/S-phase transition. However, the robustness of AMPK-dependent regulation on a myriad of fundamental cellular processes in response to metabolic stress suggests the presence of additional regulatory steps coupling AMPK and cell-cycle progression, and the molecular mechanisms behind these unrevealed regulatory steps remain to be explored.

The G₂/M-phase transition is driven by a series of tightly regulated and coordinated signaling events that eventually lead to the activation of CDC2-cyclin B (37–40). Among these events, the rate-limiting step in directing mitosis entry is the activation of dual-specificity protein phosphatase CDC25C. The activation of CDC25C generally involves two steps, initiation and amplification (41, 42). The latter requires an array of protein kinases that can extensively phosphorylate CDC25C and change its conformation (43–50). Likewise, the initiation step of CDC25C activation requires multiple coordinated events, including dephosphorylation of serine 216, a conserved inhibitory phosphorylation, dissociation from the inhibitor 14-3-3, and change in the subcellular location (51–55). The amplification step of CDC25C activation is part of a positive-feedback loop that enables a rapid, robust, and irreversible mitosis entry, whereas the initiation step represents a surveillance mechanism that ensures the order and integrity of the cell-cycle machinery (56). Supporting this idea, the DNA damage-induced G₂-phase checkpoint is largely mediated through inhibition of CDC25C, thus suppressing CDC2-cyclin B. Importantly, this is a p53-independent mechanism that is critical for the DNA damage response in most cancer cells because p53 loss of function is common in cancer cells (57–60). Because metabolic stress also causes cell-cycle arrest, it is conceivable that CDC25C may also represent a critical target of the metabolic checkpoint on cell-cycle progression.

In this study, we report a crucial role of AMPK in regulating the G₂/M-phase transition. Unlike AMPK-dependent regulation on the G₁/S transition, AMPK activation delays mitosis entry independently from its regulation on p21, p27, and mTORC1. Instead, AMPK directly phosphorylates CDC25C on serine 216, an inhibitory phosphorylation event that has been previously shown to retain CDC25C in the cytosol and keep it inactive (51, 53, 54, 61, 62). Either acute overexpression of CDC25C-S216A mutant or inhibition of WEE1 can reverse cell-cycle G₂-phase arrest imposed by AMPK activation. Moreover, pharmacologic abrogation of AMPK-mediated cell-cycle arrest by WEE1 inhibitor induces cell death. These findings reveal a novel AMPK-dependent metabolic checkpoint on cell-cycle G₂/M transition, and pharmacological abrogation of this checkpoint may represent a new therapeutic approach to treat cancers.

Results and discussion

Activation of AMPK at G₂ phase delays mitosis entry

Previous studies have demonstrated an AMPK-dependent cell-cycle checkpoint at the G₁/S-phase boundary, which may ensure the coordination of DNA synthesis in S phase with the availability of nutrients for nucleotide biosynthesis in G₁ phase (27, 33). However, it is still unclear whether the G₂/M-phase transition is regulated by AMPK and represents a checkpoint for the coordination of cell metabolism and cell-cycle progression. For this, we treated HeLa cells overnight with two mechanistically distinct pharmacologic activators of AMPK, 5-aminoimidazole-4-carboxamide 1- β -D-ribofuranoside (AICAR) or A 769662 (A7) (63). AICAR is considered as an AMP-mimetic compound that directly binds to a nucleotide-binding pocket in the AMPK α subunit and promotes AMPK kinase activities; A7 binds to a cleft between the AMPK α and β subunits and causes allosteric activation of the AMPK kinase complex (63–66). We found that both AICAR and A7 increased the percentage of cells in the G₁ and G₂ phases, as indicated by PI staining in combination with BrdU incorporation (Fig. 1A). By contrast, the percentage of cells in mitosis indicated by phosphorylation of histone H3 (*pH3*) is reduced following AICAR and A7 treatment (Fig. 1A). Notably, the disappearance of BrdU incorporation in AICAR group is probably due to the substrate competition between BrdU and AICAR, both of which are nucleotide analogs. Next, we repeated the experiment in the presence of nocodazole, a reversible inhibitor of microtubule polymerization, which blocks mitosis exit and therefore highlights the changes of mitotic entry following treatments. Both AICAR and A7 reduced the percentage of cells in mitosis compared with the control group (Fig. 1B).

We next applied radiochemical-based approaches to determine the activity of major catabolic pathways that could fuel the biosynthetic programs in cells released into G₁ phase or G₂ phase. We also included cells starved by serum removal as a control to indicate the baseline metabolic activity. Compared with cells at G₁ phase or serum-starved cells, cells at G₂ phase significantly up-regulated glycolysis, indicated by the detritiation of [5-³H]glucose; glucose consumption via the pentose phosphate pathway (PPP), indicated by ¹⁴CO₂ release from [1-¹⁴C]glucose; and glutamine consumption through oxidative catabolism (glutaminolysis), indicated by ¹⁴CO₂ release from [U-¹⁴C]glutamine (Fig. 2A). In contrast, both mitochondria-dependent pyruvate oxidation through the tricarboxylic acid (TCA) cycle, indicated by ¹⁴CO₂ release from [2-¹⁴C]pyruvate, and fatty acid β -oxidation, indicated by the detritiation of [9,10-³H]palmitic acid, were comparable among all three groups (Fig. 2B). These data suggest that cells at G₂ phase actively engage glucose and glutamine catabolic programs to meet their bioenergetic and biosynthetic demands.

Next, we sought to determine whether the acute activation of AMPK at G₂ phase would cause a delay of mitosis entry. This would determine whether the delay of mitosis entry is a secondary effect from the G₁/S-phase transition in the presence of AMPK activators. For this, we first synchronized cells at the G₁/S boundary by double thymidine blockage and then released the cells into S phase and treated them with AMPK activators

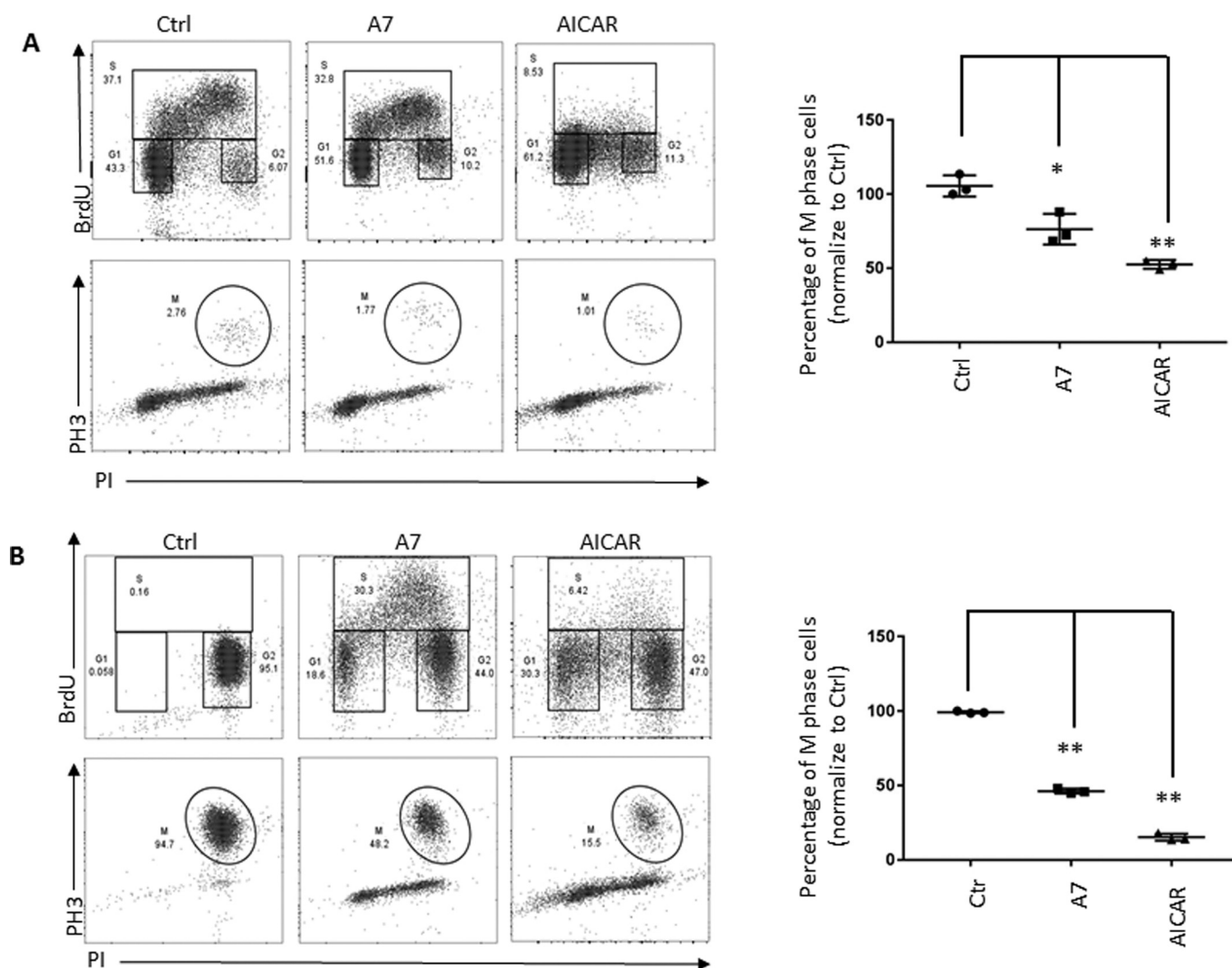


Figure 1. Pharmacologic activation of AMPK increases the percentage of cells in G₁ and G₂ phase. *A*, HeLa cells were treated with 300 μ M A7 or 2 mM AICAR for 14 h before harvesting the samples. The percentage of cells in G₁, S and G₂ phase is indicated by PI staining in combination with BrdU incorporation (top). The percentage of cells in mitosis (M) is indicated by phosphorylation of histone H3 (pH3, bottom). The scatter plot indicates the percentage of M-phase cells treated with AMPK activator, and the percentage of M-phase cells in vehicle-treated cells was set to 100. Error bars, S.D. of triplicate samples. *B*, HeLa cells were treated with 300 μ M A7 or 2 mM AICAR in combination with 100 ng/ml nocodazole for 14 h. The percentage of cells in G₁, S, and G₂ phase is indicated by PI staining and BrdU incorporation (top). The percentage of M-phase cells is indicated by phosphorylation of histone H3 (pH3, bottom). The scatter plot indicates the percentage of M-phase cells treated with AMPK activator, and the percentage of M-phase cells in vehicle-treated cells was set to 100. Error bars, S.D. of triplicate samples. *, $p < 0.05$; **, $p < 0.01$.

and nocodazole once they reached G₂ phase (Fig. 3A). In addition to AICAR and A7, we also included metformin and phenformin, two respiration chain complex I inhibitors, to indirectly activate AMPK by suppressing ATP production (67). Our results clearly showed that these AMPK activators reduced the percentage of cells in mitosis in a dose-dependent manner (Fig. 3, B and C). Moreover, none of the acute treatment with these compounds caused significant apoptosis, as measured by PI uptake and cell-surface annexin V staining (Fig. S1). Collectively, our results suggest that activation of AMPK in cells at G₂ phase delays mitosis entry.

DNA damage pathway and mTOR pathway are not involved in mediating AMPK-dependent regulation on G₂/M-phase transition

It has been well-established that cells in G₂ phase with damaged DNA are prevented from entering into mitosis, and the

control mechanisms behind this are known as the G₂ checkpoint (60, 68–71). To determine whether activation of AMPK cross-talks with the DNA damage pathway and causes G₂ arrest, we treated cells with AICAR at G₂ phase and examined molecules involved in the DNA damage response pathways in cells collected at various time points. Doxorubicin, a reagent that causes DNA adducts and activates the DNA damage response, readily induced phosphorylation of checkpoint kinase 1 (Chk1) and histone H2AX (H2AX), two characteristic biomarkers of the DNA damage response (72). However, treatment with AICAR failed to induced any visible phosphorylation of Chk1 and H2AX (Fig. 4A). Previous studies have demonstrated that AMPK phosphorylates p53 and causes the accumulation of p21, a transcriptional target of p53 that mediates p53-dependent regulation on cell cycle (28, 73–75). In a different cellular context, AMPK was reported to regulate p27 and induce autophagy (29). Both p21 and p27 are CDK inhibitors

AMPK phosphorylates CDC25C and regulates mitosis entry

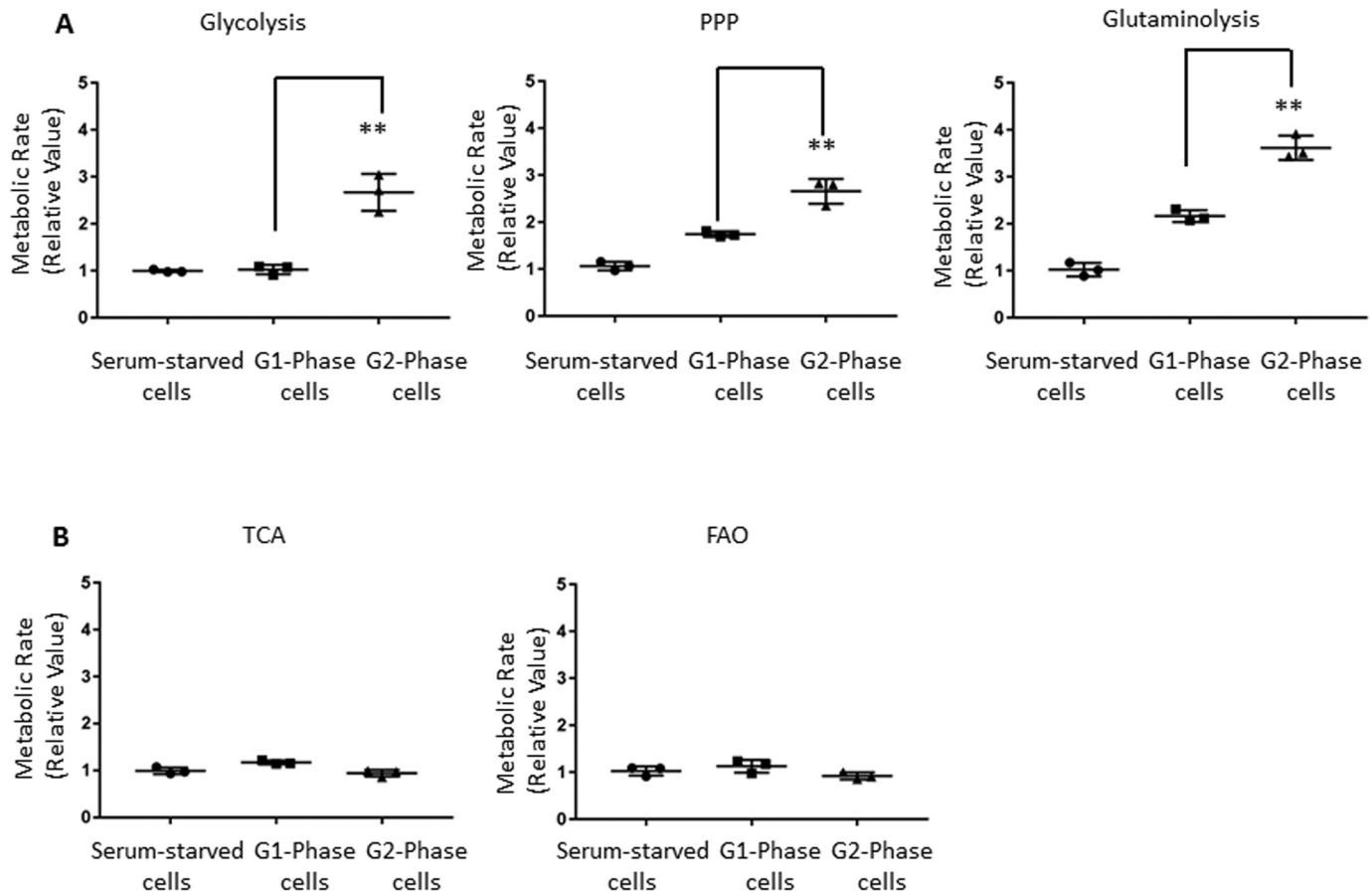


Figure 2. Cells display heightened glucose and glutamine catabolism in G₂ phase. A, HeLa cells were released into G₁ phase after mitotic shake-off or were release into G₂ phase after double-thymidine arrest. Unsynchronized HeLa cells incubated in medium without serum for 6 h before the assay were used as control for the baseline metabolic activity. The indicated metabolic activities were determined by measuring the generation of ³H₂O from [1-¹⁴C]glucose (glycolysis; left) or the generation of ¹⁴CO₂ from [1-¹⁴C]glucose (PPP; middle) or from [U-¹⁴C]glutamine (glutaminolysis; right). Metabolic rate was normalized to serum-starved cells. Error bars, S.D. of triplicate samples. B, indicated metabolic activities were determined by measuring the generation of ¹⁴CO₂ from [2-¹⁴C]pyruvate (TCA; left) and measuring the generation of ³H₂O from [9,10-³H]palmitic acid (fatty acid β -oxidation; right). Metabolic rates were normalized to control. Error bars, S.D. of triplicate samples. **, $p < 0.01$.

and play critical roles in cell-cycle regulation (76, 77). However, we have found that the treatment with AICAR failed to induce the expression of p21 or p27 (Fig. S2). Our findings are also consistent with earlier reports showing no detectable p53 protein in HeLa cells (78, 79).

It has also been reported that AMPK regulates cell-cycle progression through directly inhibiting mTORC1 complex, which is the central player in sensing nutrients and coordinately regulating cell-cycle progression (31, 33–36). To determine whether mTORC1 is involved in mediating AMPK-dependent regulation on G₂/M transition, we treated cells with either AMPK activators or mTORC1 inhibitors at G₂ phase and examined the phosphorylation of mTORC1 effector molecules, P70 kinase and ribosomal protein S6, in cells collected at the time when control cells start entering into mitosis. Whereas A7 treatment and the mTORC1 inhibitor treatments led to the suppression of mTORC1, as indicated by the loss of phosphorylation of P70 kinase and S6, AICAR treatment failed to suppress mTORC1 activities (Fig. 4B). Importantly, neither rapamycin nor torin treatment delayed mitosis entry (Fig. 4C). Collectively, these findings suggested that mTORC1 is not involved in mediating AMPK-dependent regulation of the G₂/M transition.

AMPK phosphorylates CDC25C at serine 216 in vitro and in cells

The activity of CDKs oscillates throughout the cell cycle and determines the transition between different cell-cycle phases (76, 77). Mitosis entry is driven by CDC2-cyclin B, which is coordinately regulated by CDC25, WEE1, and MYT1. WEE1 and MYT1 phosphorylate and keep CDC2-cyclin B inactive in G₂ phase. CDC25 activates CDC2-cyclin B and drives cells into mitosis by dephosphorylating the inhibitory phosphorylation sites on CDC2-cyclin B (Fig. 5A). Given that the mitotic regulators mentioned above are all regulated by phosphorylation and AMPK is a signaling protein kinase, we asked whether AMPK is capable of directly phosphorylating and modulating any of the above mitotic regulators. Previous studies have revealed the optimal consensus phosphorylation motif for AMPK (33, 80). We therefore applied a bioinformatics tool (Scansite3 (81)) to search for putative AMPK-mediated phosphorylation motifs in CDC25C, WEE1, MYT1, CDC2, and cyclin B1. The inspection of these protein sequences revealed one putative AMPK phosphorylation site, serine 216, in CDC25C (Fig. 5B). The phosphorylation of serine 216 plays a key role in the temporal and spatial regulation of CDC25C and

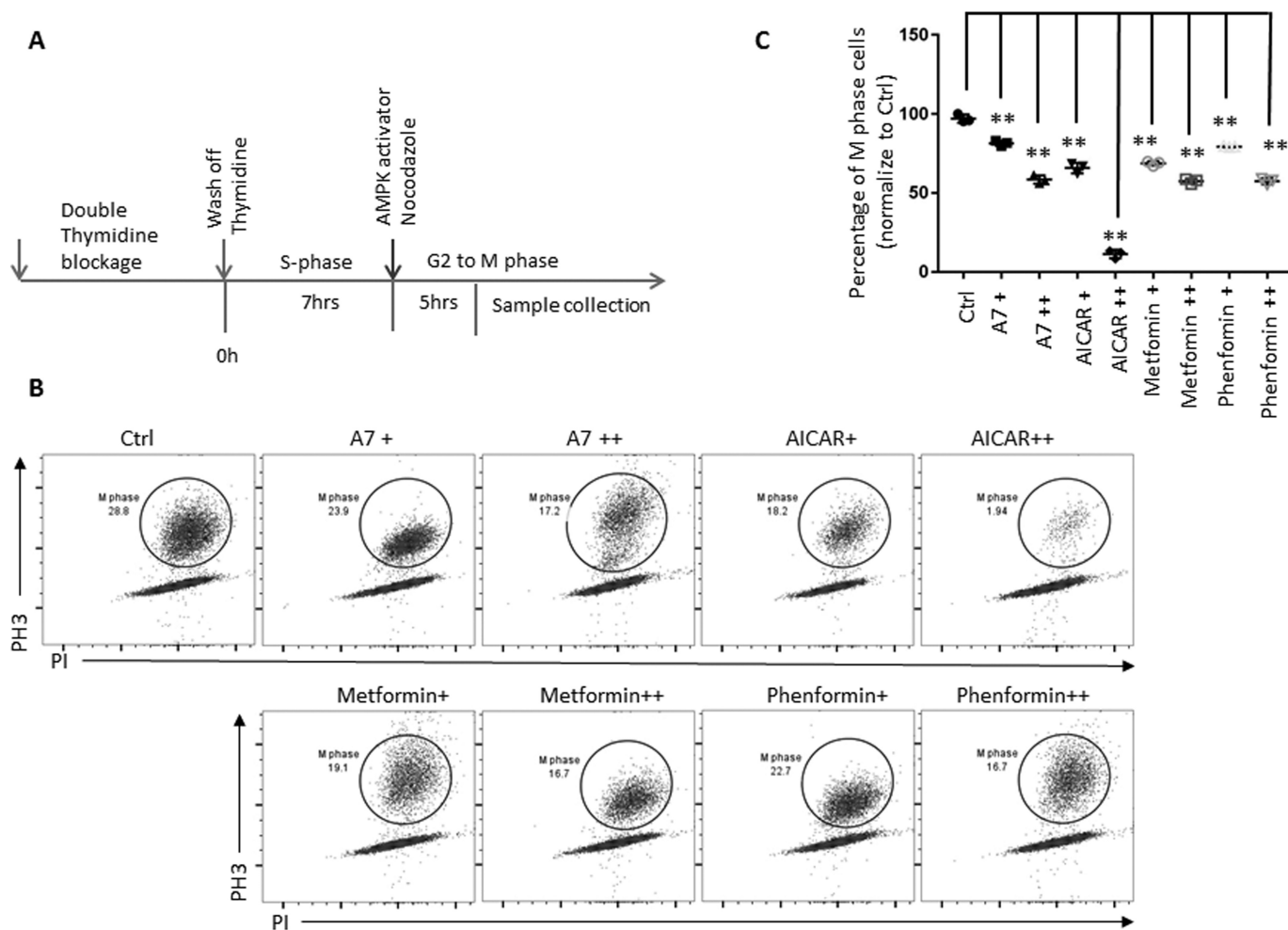


Figure 3. Acute activation of AMPK at G₂ phase delays mitosis entry. *A*, schematic view of cell synchronization and the indicated treatments. Representative flow cytometric dot plots (*B*) and the scatter plot (*C*) indicate the percentage of M-phase cells treated with indicated compounds at G₂ phase (A7+, 150 μM; A7++, 300 μM; AICAR+, 2 mM; AICAR++, 4 mM; metformin+, 2 mM; metformin++, 4 mM; phenformin+, 20 μM; phenformin++, 100 μM). The percentage of M-phase cells in vehicle-treated cells was set to 100. Error bars, S.D. of triplicate samples. **, *p* < 0.01.

the G₂/M transition in response to DNA damage and during normal cell-cycle progression (51, 53, 54, 61, 62). To validate serine 216 as an AMPK phosphorylation site in CDC25C, we took an integrated stepwise approach. We first transfected cells with constructs expressing either WT or mutant CDC25C (serine to alanine/S216A) fused to the Myc epitope tag (Myc-CDC25C), immunoprecipitated CDC25C with anti-Myc epitope tag antibodies, and then immunoblotted the protein samples using a phosphorylation-specific antibody that recognizes the phosphorylated AMPK consensus motif (33, 80). Whereas the phospho-AMPK substrate motif antibody recognized WT CDC25C, the S216A mutation abolished such recognition, suggesting that Ser-216 is within the AMPK substrate motif in CDC25C (Fig. S3A). Second, we generated recombinant CDC25C fused to glutathione *S*-transferase (GST-CDC25C) and a non-related GST-tagged protein and phosphorylated these proteins with recombinant AMPK or extracellular signal-regulated kinase 1 (ERK1) or PBS control. ERK readily phosphorylated CDC25C at threonine 48, as we reported previously (49). However, only the AMPK-mediated phosphorylation site in CDC25C was recognized by the phospho-AMPK substrate motif antibody or the pSer-216 antibody (Fig. 5C).

Third, we treated cells with AICAR or transfected cells with either a control construct or a construct expressing a constitutively active mutant of the AMPK catalytic subunit (AMPK-CA) (82) and then immunoblotted with the pSer-216 antibody. Both pharmacologic and genetic activation of AMPK readily enhanced the phosphorylation of Ser-216 in CDC25C (Fig. 5D and Fig. S3B). Finally, we applied a chemical genetic approach to validate Ser-216 in CDC25C as a genuine AMPK-mediated phosphorylation site in cells (83–85). This approach is based on the concept that protein kinase can only use ATP as a phosphate donor; however, the point mutation of a conserved gate-keeper residue in the ATP-binding pocket of a protein kinase would allow mutant protein kinase (analog-specific (AS)) to utilize ATP analog (ATPγS) as a phosphate donor. The specific labeling of kinase substrate with thiophosphate (thioP), followed by protein immunoprecipitation and alkylation, would enable the recognition of AS mutant-dependent phosphorylation with a thioP-specific antibody. This approach has been applied to identify direct substrates of various protein kinases, including AMPK (83, 86). Thus, we co-transfected cells with a construct expressing Myc-tagged CDC25C as well as a construct expressing either FLAG-tagged WT or AS-AMPK and

AMPK phosphorylates CDC25C and regulates mitosis entry

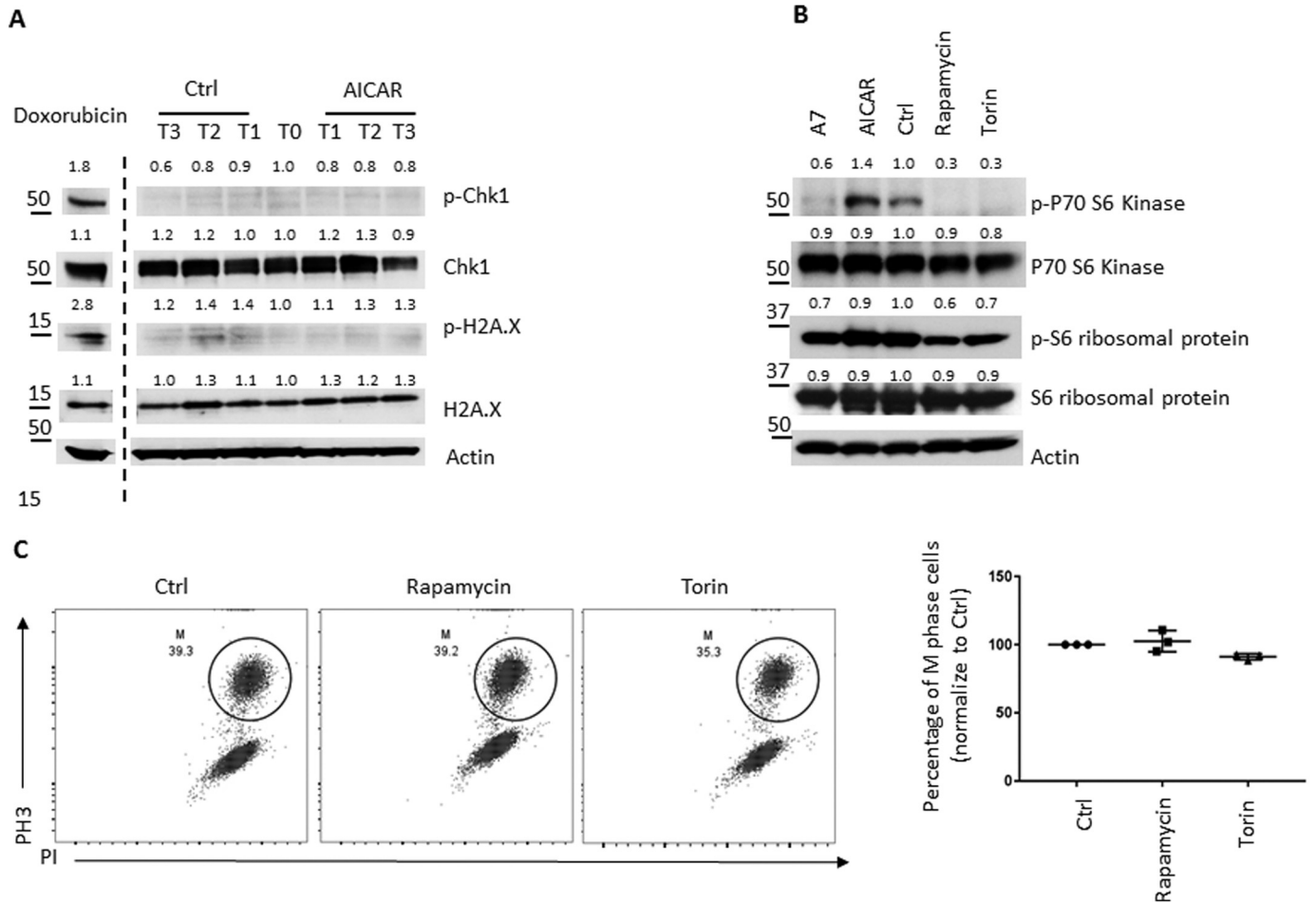


Figure 4. Pharmacological activation of AMPK on cells in G₂ phase does not activate the DNA damage pathway or suppress the mTOR pathway. A, HeLa cells were treated with or without 2 mM AICAR at G₂ phase alone with nocodazole. Cells were collected at different time points (T0, 7 h after the second thymidine release when AMPK activators and nocodazole were added; T1, 2 h after T0; T2, 4 h after T0; T3, 6 h after T0). The level of the indicated proteins in HeLa cells was determined by immunoblotting. Doxorubicin (1 μg/ml), as a DNA damage-inducing agent, was included as a positive control. B, HeLa cells were treated with 300 μM A7, 2 mM AICAR, 200 nM rapamycin, or 2 μM torin at G₂ phase alone with nocodazole. Cells were collected 12 h after the second thymidine release. The level of the indicated proteins in HeLa cells was determined by immunoblot. C, the percentage of M-phase cells with the indicated treatments was determined by p-H3 staining. The representative flow cytometric dot plots (left) and scatter plot (right) indicate the percentage of M-phase cells in different groups. The percentage of M-phase cells in vehicle-treated cells was set to 100. Error bars, S.D. of triplicate samples.

showed that Myc-tagged CDC25C could be labeled with thioP only in the presence of AS-AMPK (Fig. 5E). Then we followed up the above experiment by co-transfecting cells with a construct expressing AS-AMPK as well as a construct expressing either Myc-tagged WT or S216A CDC25C. The recognition by thioP-specific antibody was significantly compromised by S216A mutation (Fig. 5F), suggesting that Ser-216 is a direct phosphorylation site and very likely the only phosphorylation site of AMPK on CDC25C.

Acute modulation of CDC25C or WEE1 partially relieves AMPK-dependent inhibition of the G₂/M-phase transition

Our data on AMPK-dependent phosphorylation of Ser-216 on CDC25C suggested that AMPK suppresses the G₂/M-phase transition through the phosphorylation and inhibition of CDC25C. CDC25C activates CDC2-cyclin B and promotes the G₂/M-phase transition by antagonizing WEE1 (*i.e.* by dephosphorylating WEE1-dependent phosphorylation sites on CDC2-cyclin B) (42, 87, 88). We therefore reasoned that the abrogation of WEE1 or the abrogation of Ser-216 on CDC25C would

relieve AMPK-dependent inhibition of the G₂/M-phase transition (Fig. 6A). To test this, we first took a pharmacological approach, using MK1775, to block WEE1 activity in the presence of AMPK activators. MK1775 is a potent WEE1 inhibitor and allows us to acutely block WEE1 activity in cells synchronized at G₂ phase without interfering with the cell-cycle synchronization process (89). Because a pharmacological inhibitor readily suppresses its target upon addition, we treated cells with MK1775 at the same time as we added AMPK inhibitors, ensuring a minimal perturbation by the compound on G₂-phase progression (Fig. 6B). Supporting the idea that the inhibition of WEE1 may antagonize AMPK-mediated suppression on CDC25C, neither A7 nor AICAR treatment delayed mitosis entry in the presence of MK1775; however, A7 and AICAR treatment consistently reduced the percentage of cells in mitosis in the absence of MK1775 (Fig. S4, A and B). Next, we applied a genetic approach to knock down WEE1 by transfecting a WEE1-specific siRNA. To avoid perturbing the normal cell-cycle progression following a long-term WEE1 knock-

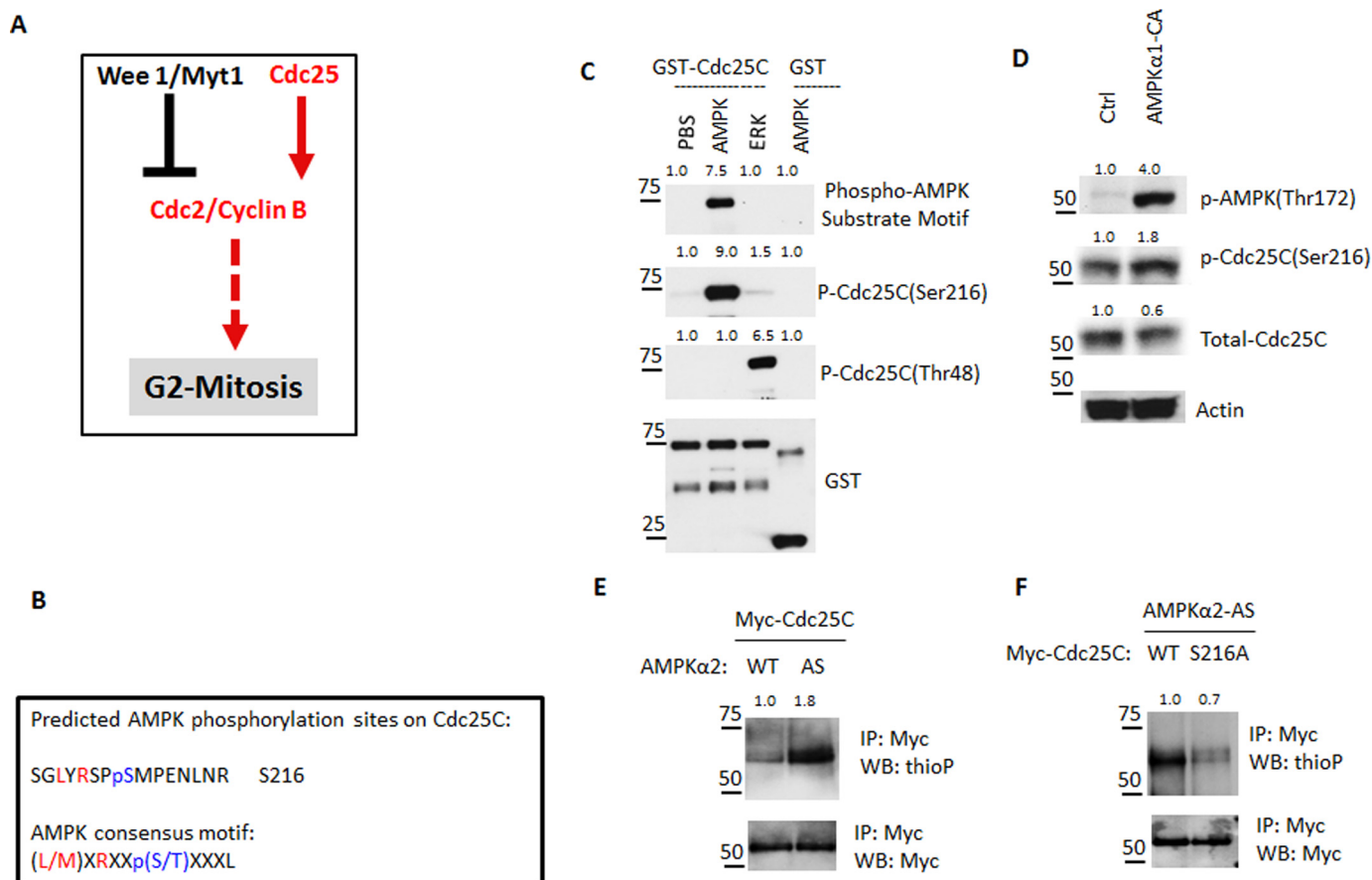


Figure 5. AMPK phosphorylates CDC25C at serine 216 *in vitro* and in cells. *A*, model showing that G₂/M-phase transition is regulated by CDC25C and WEE1. *B*, potential AMPK phosphorylation motif of CDC25C was predicted by Scansite3. The AMPK consensus phosphorylation motif and the predicted motif are shown in *single-letter amino acid code*. Positions marked as *red* showed the similarity between the two motifs, and the predicted phosphorylation site of CDC25C is marked as *blue*. *C*, bacterially expressed GST-CDC25C or GST was incubated with recombinant AMPK or ERK in an *in vitro* phosphorylation assay. Proteins were resolved by SDS-PAGE and immunoblotting for the indicated antibodies. *D*, HeLa cells were transfected with a construct expressing a constitutively active mutant of the AMPK catalytic subunit (AMPK-CA) or a blank control plasmid for 2 days, and the expression of the indicated proteins in transfected cells was determined by immunoblot. *E*, analog-sensitive kinase assay in cells. HeLa cells were transfected with Myc-CDC25C together with either WT-AMPK α 2 or AS-AMPK α 2 and treated with ATP γ S analog as a phosphodonor. CDC25C was immunoprecipitated (IP) with Myc tag antibody and blotted (WB) with the indicated antibodies. *F*, analog-sensitive kinase assay in cells. HeLa cells were transfected with AS-AMPK α 2 together with either WT or S216A mutant Myc-CDC25C and treated with ATP γ S analog as a phosphodonor. CDC25C was immunoprecipitated with Myc tag antibody and blotted with the indicated antibodies.

down, we transfected cells with WEE1 siRNA when synchronized cells were released into S phase and collected samples 12 h later to examine the protein level of WEE1 and cell-cycle status (Fig. 6B). The protein level of mammalian WEE1 oscillates during the cell cycle and thus indicates a short half-life of WEE1 protein. This allows us to deplete WEE1 in a short time frame by siRNA (Fig. 6C) (90–92). Consistent with our data on MK1775, siRNA-mediated acute knockdown of WEE1 also partially relieved AMPK-mediated suppression of the G₂/M transition (Fig. 6C and Fig. S4C). Last, we sought to genetically modulate the phosphorylation of Ser-216 on CDC25C and examine its effect on G₂/M-phase transition in the context of AMPK activation. To minimize the perturbation of constitutive overexpression of CDC25C on normal cell-cycle progression, we established a cell line stably expressing a doxycycline-inducible CDC25C (S216A) mutant, which enables the acute induction of CDC25C (S216A) following doxycycline treatment when synchronized cells were released into S phase (Fig. 6B). We confirmed the acute induction of CDC25C (S216A) by immunoblotting and showed that such treatment partially

relieved AMPK-mediated suppression of the G₂/M-phase transition (Fig. 6D and Fig. S4D). Of note, neither the WEE1 siRNA nor the induction of CDC25C (S216A) in the context of AMPK activation caused additional stresses and induced cell death during the time frame of experiments (Fig. S5). Taken together, our results suggest that AMPK-mediated phosphorylation of Ser-216 on CDC25C represents a mechanism of cell-cycle checkpoint.

WEE1 inhibitor synergizes with AMPK activators to induce cell death

AMPK is a central sensor of cellular energy status and therefore plays a key role in maintaining metabolic and bioenergetic homeostasis (26, 93). We envisioned that AMPK-mediated suppression on G₂/M-phase transition may represent a metabolic checkpoint that ensures the coordination of sequential cell-cycle transitions with metabolic status. As such, abrogation of the checkpoint may reduce the ability of cells to survive. To test this idea, we treated cells with AMPK activator, WEE1 inhibitor, or a combination of these two and monitored the cell

AMPK phosphorylates CDC25C and regulates mitosis entry

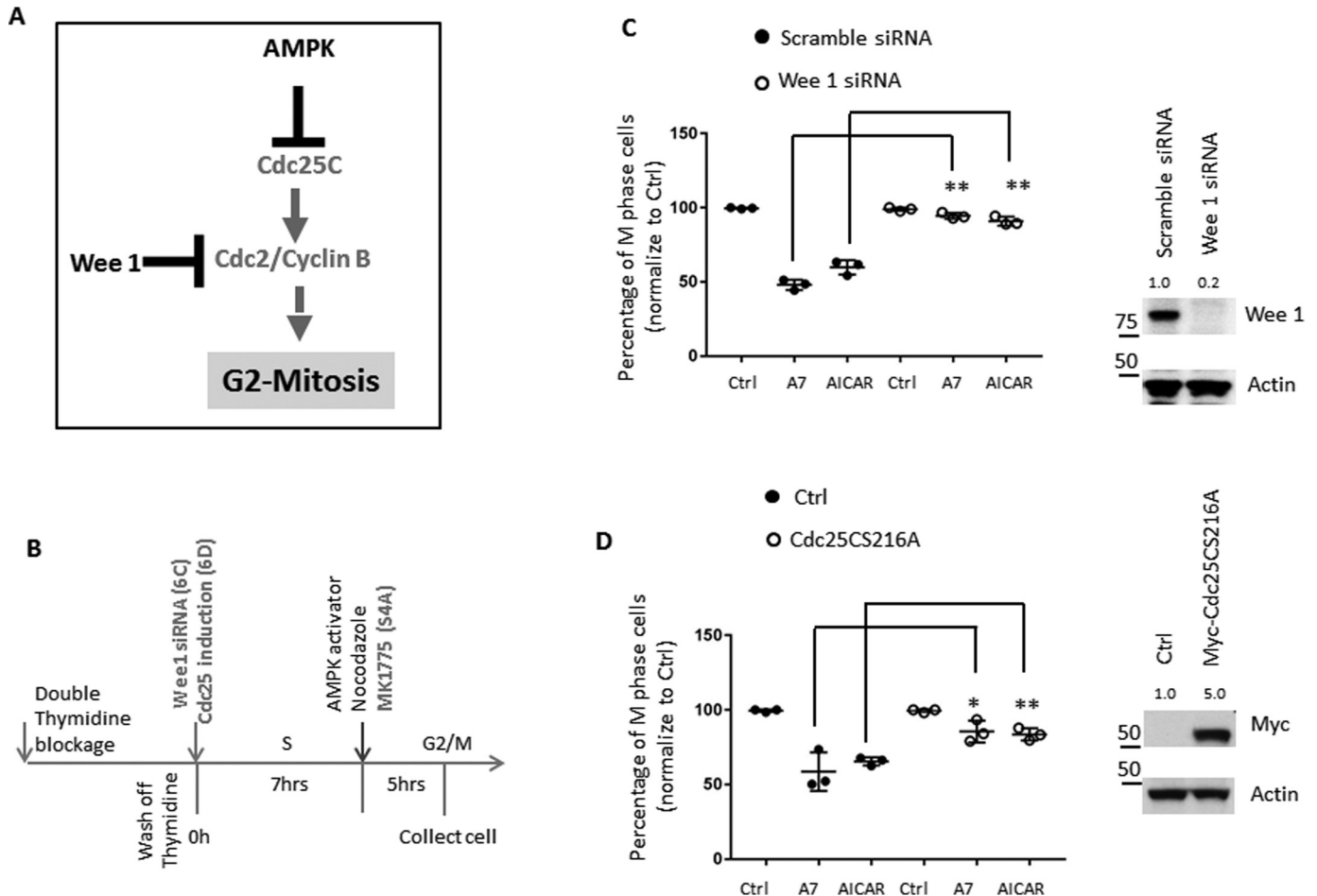


Figure 6. Acute induction of CDC25C or suppression of WEE1 partially reverses the effect of AMPK activation on the G₂/M-phase transition. *A*, model showing that the G₂/M-phase transition is regulated by CDC25C and WEE1. *B*, schematic view of cell synchronization and the indicated treatments. Synchronized HeLa cells that stably express reverse tetracycline-controlled transactivator and doxycycline-inducible CDC25C were treated with doxycycline when cells were released from the second thymidine block (G₁/S boundary). Synchronized HeLa cells were transfected with WEE1 siRNA at the G₁/S boundary or treated with WEE1 inhibitor at G₂ phase (7 h after cells were released from the second thymidine block), respectively. AMPK activators and nocodazole were added when cells are in G₂ phase. *C*, the percentage of M-phase cells in HeLa cells transfected with scramble siRNA or WEE1 siRNA was determined by phosphorylation of histone H3 (pH3) staining. The percentage of M-phase cells in vehicle-treated cells was set to 100, and the value of AMPK activator-treated cells was normalized to that of vehicle-treated cells. Error bars, S.D. of triplicate samples (left). Cell lysates were blotted with the indicated antibodies (right). *D*, the percentage of M-phase cells in HeLa cells that stably express reverse tetracycline transcriptional activator (Ctrl) or CDC25C-S216A following doxycycline treatment was determined by phosphorylation of histone H3 (pH3) staining. The percentage of M-phase cells in vehicle-treated cells was set to 100, and the value of AMPK activator-treated cells was normalized to that of vehicle-treated cells. Error bars, S.D. of triplicate samples (left). Cell lysates were blotted with the indicated antibodies (right). *, $p < 0.05$; **, $p < 0.01$.

growth curve. Whereas single-agent treatment demonstrated a moderate ability to suppress cell growth, either A7 or AICAR in combination with MK1175 led to a synergistic effect on suppressing cell growth (Fig. 7A). Moreover, the growth suppression correlated with cell death induction, as measured by cell surface staining of annexin V and cellular uptake of PI, following the treatment with these reagents (Fig. 7B). Our studies suggest that abrogation of AMPK-dependent G₂ checkpoint response induces cell death and may represent an attractive cancer therapeutic strategy.

Metabolic stress suppresses the G₂/M transition partially through AMPK

We next sought to assess the impact of metabolic stress on AMPK and cell-cycle G₂/M transition. We first applied glucose-free conditional medium and hexokinase inhibitor, 2-deoxyglucose (2DG), to induce an acute metabolic stress and

assess the activation of AMPK. Given that the average duration of G₂ phase is between 2 and 5 h, we reasoned that the acute condition (1 h) is more relevant to assess the impact of metabolic stress on cell-cycle G₂/M transition. Under this condition, we found that U2OS cells but not HeLa cells respond to acute metabolic stress by enhancing AMPK activity, as indicated by the increase of AMPK autophosphorylation and phosphorylation of ACC (Fig. 8A). Previous studies have shown that HeLa cells are deficient in liver kinase B1 (LKB1), an AMPK-activating kinase (94), and we have also confirmed LKB1 deficiency in HeLa cells by Western blotting (Fig. 8B). LKB1 deficiency probably renders HeLa cells resistant to metabolic stress-induced activation of AMPK because AMP/ADP promotes the conformational change of AMPK that will facilitate the phosphorylation by LKB1 and consequentially enhance AMPK activity (95, 96). As such, we chose U2OS cells to further assess the impact of metabolic stress on AMPK and on the G₂/M transition. For

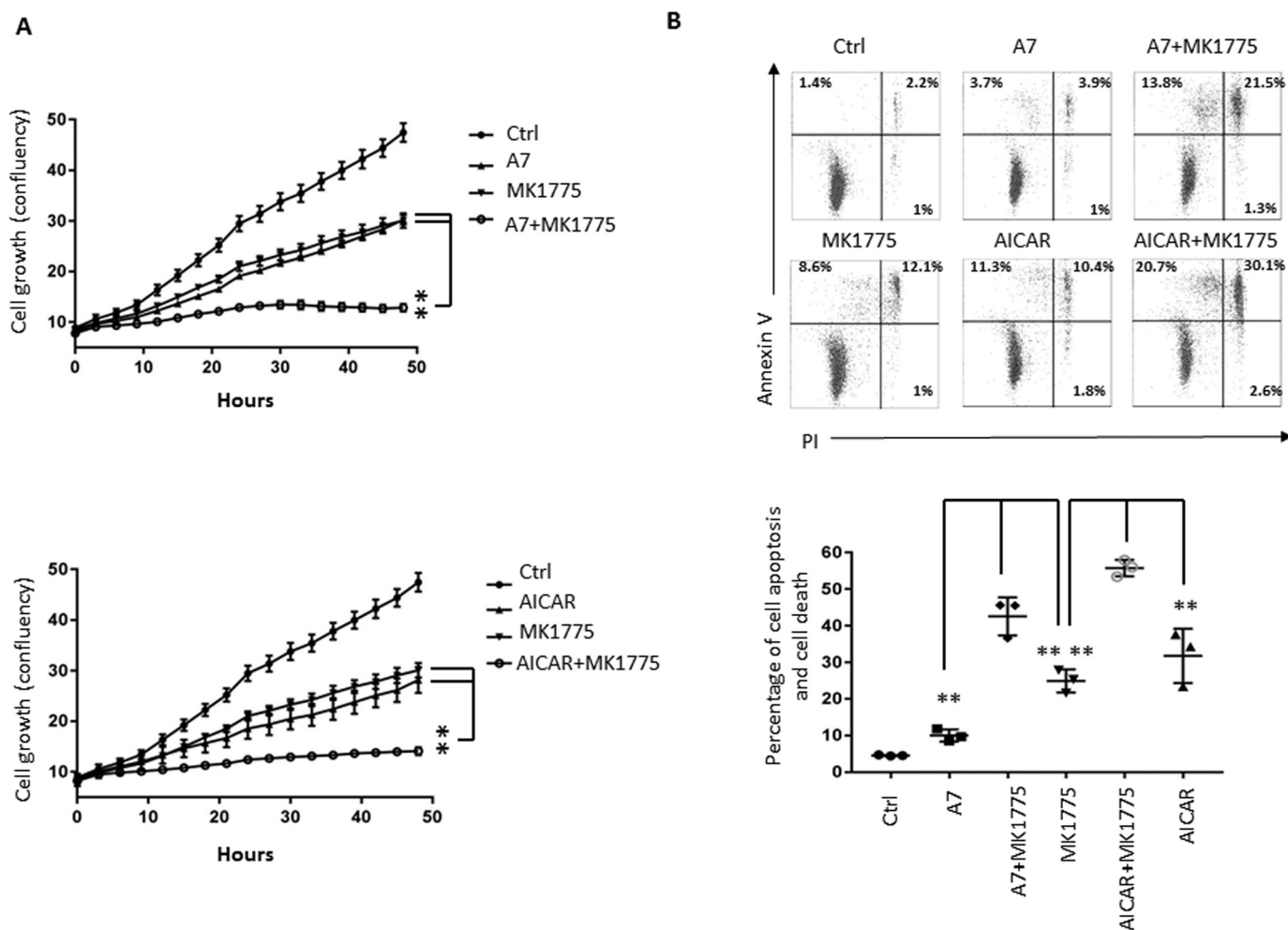


Figure 7. Pharmacological ablation of G₂ checkpoint synergizes with AMPK activators to induce cell death. A, HeLa cells were treated with AMPK activators, MK1775, or a combination of the two, and the growth curve was determined by live cell image analysis (IncuCyte ZOOM™). Error bars, S.D. of quadruplicate samples. B, HeLa cells were treated with AMPK activators, MK1775, or a combination for 48 h, and cell death was determined by staining with FITC-conjugated annexin V and PI followed by FACS analysis. The percentage of apoptotic and dead cells was determined from three experiments. Bars, mean ± S.D. **, $p < 0.01$.

this, we applied siRNA to transiently knock down AMPK α 1 in U2OS cells (Fig. 8C). Both the procedure of transient transfection and the time frame (48 h) required to achieve an efficient knockdown of AMPK α 1 interfered with the standard protocol for double thymidine synchronization. We therefore chose to treat cells with the indicated siRNA for 48 h and then applied nocodazole, to hold cells in mitosis, with or without metabolic stress. As Fig. 8D shows, metabolic stress imposed by either glucose starvation or glycolysis inhibitor 2DG significantly suppressed the percentage of cells entering into mitosis following nocodazole treatment. Importantly, AMPK α 1 knockdown partially relieved metabolic stress-mediated suppression on the G₂/M-phase transition (Fig. 8D). Collectively, our results suggested that acute metabolic stress (nutrient starvation or metabolic inhibitor) activates AMPK and suppresses the G₂/M-phase transition.

Cell-cycle checkpoints are critical surveillance mechanisms that monitor the integrity and fidelity of genome replication and separation and thus ensure the order and timely execution of cell-cycle transitions (97–99). In addition, mammalian cells have evolved to rapidly respond to changes of internal meta-

bolic status and external nutrient levels by engaging a mechanism of adaptation, which requires robust molecular machineries that sense metabolic signals. The consequences of such adaptation include not only metabolic rewiring but also commitments on cell-cycle progression, cell death, and many other basic or specialized cellular functions (100–102). Previous studies have shown that AMPK is crucial for the survival of cells by acting on an array of signaling and biochemical pathways to rapidly restore the energy status upon a variety of metabolic stresses (25, 26). Our studies implicate AMPK as a critical signaling node that interconnects with cell-cycle machinery through a direct phosphorylation and suppression of CDC25C. This allows cells to constantly inspect the metabolic status, halt the cell-cycle progression upon perturbations, and therefore ensure the cellular metabolic fitness and homeostasis of the progenies. Our studies further suggest that phosphorylation of Ser-216 in CDC25C is not only an evolutionarily conserved mechanism in normal cell-cycle regulation, but also a shared G₂-phase checkpoint mechanism in mammalian cells in response to both DNA damage and metabolic stress (51, 53, 54, 61, 62). These findings together support the idea that some key

AMPK phosphorylates CDC25C and regulates mitosis entry

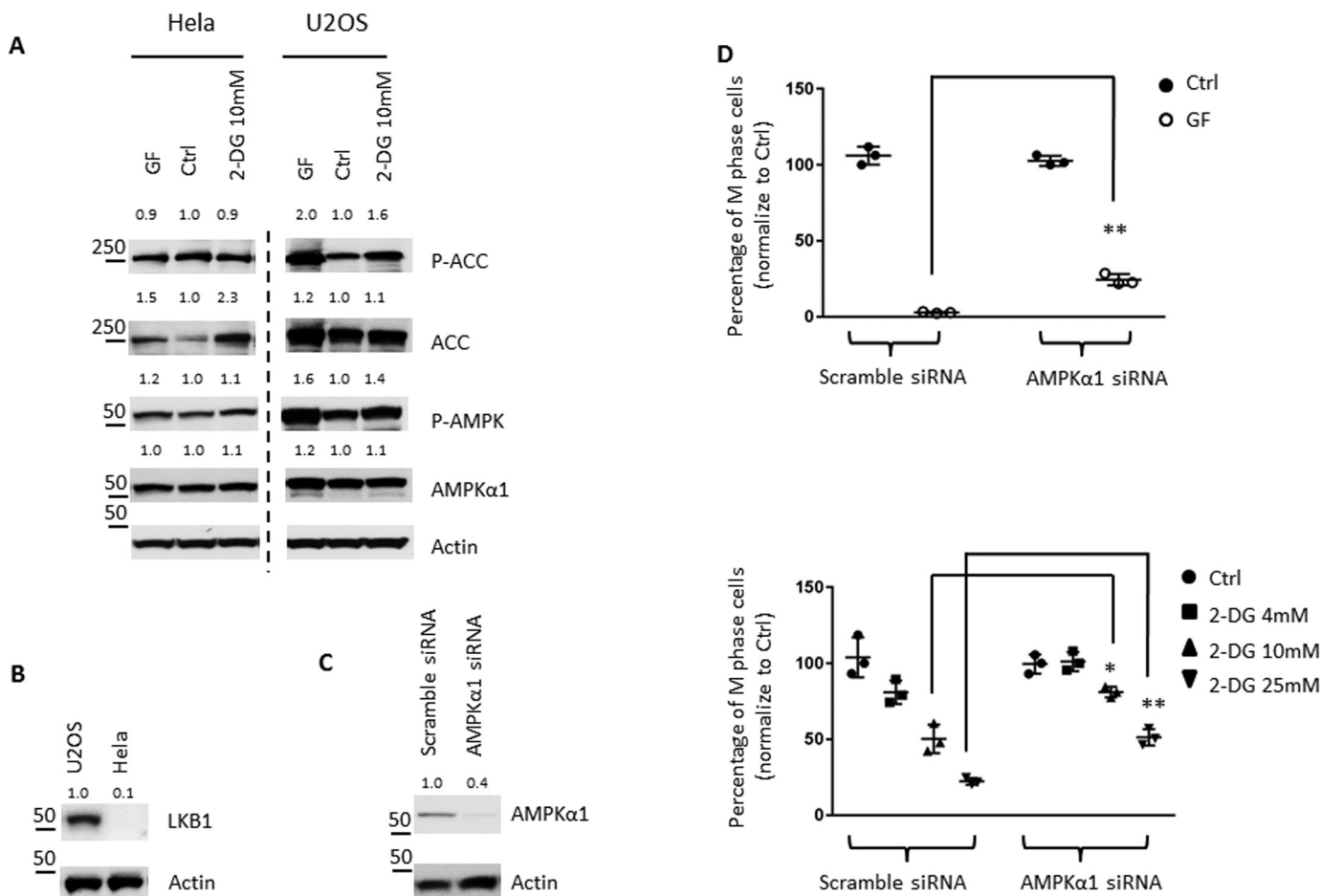


Figure 8. Metabolic stress suppresses G₂/M transition partially through AMPK. *A*, U2OS and HeLa cells were cultured in glucose-free medium or treated with 10 mM 2DG for 1 h. The level of the indicated proteins in cells was determined by immunoblotting. *B*, U2OS and HeLa cells were collected, and the level of the indicated proteins was determined by immunoblot. *C*, U2OS cells were transfected with scrambled siRNA or AMPKα1 siRNA for 48 h. The level of the indicated proteins in cells was determined by immunoblot. *D*, U2OS cells were transfected with scrambled siRNA or AMPKα1 siRNA for 48 h and then incubated in control or glucose-free medium (GF, top) or treated with a different concentration of 2DG (bottom) along with 100 ng/ml nocodazole for 14 h. The percentage of M-phase cells was determined by the phosphorylation of histone H3 (pH3) staining. The percentage of M-phase cells in control medium was set to 100, and the value of cells in GF medium or 2DG-treated cells was normalized to their control. Error bars, S.D. of triplicate samples.

elements of the cellular stress response pathways are shared among different stresses and are conserved across many species (103, 104). In multicellular eukaryotes, programmed cell death (apoptosis) occurs when the dose of stress exceeds tolerance limits or when adaptive pro-survival checkpoint mechanisms are eliminated (105–107). MK1775 has displayed anti-tumor activities in various preclinical models and has been evaluated in clinical trials as monotherapy and adjuvant therapy (108, 109). Our studies therefore suggest that abrogation of the metabolic checkpoint on G₂/M-phase transition by WEE1 inhibitor may lead to premature mitosis entry and consequent cell death and therefore holds promise for therapeutically targeting cancer (110–112).

Experimental procedures

Cell culture and reagents

HeLa (human cervical cancer cells, ATCC) and U2OS (human osteosarcoma cells, ATCC) were grown at 37 °C/5% CO₂ in Dulbecco's modified Eagle's medium (DMEM; Corning Cellgro, Thermo Fisher Scientific, Grand Island, NY) supplemented with 10% fetal bovine serum (Gibco-Invitrogen, Carls-

bad, CA) and 1% penicillin-streptomycin (Corning). Cell line identity was authenticated by short tandem repeat analysis. Glucose-free DMEM was supplemented with 10% (v/v) heat-inactivated dialyzed fetal bovine serum, which was made dialyzing against 100 volumes of distilled water (five changes in 3 days) using Slide-ALyzer™ G₂ dialysis cassettes with cut-through MW size 2K (Thermo Fisher Scientific) at 4 °C. AICAR, A769662, rapamycin, torin, metformin, phenformin, 2-deoxy-D-glucose, and nocodazole were purchased from Cayman Chemical (Ann Arbor, MI). MK1775 was purchased from MedKoo Biosciences (Morrisville, NC).

siRNA transfection

The siRNA oligonucleotides corresponding to human WEE1 and AMPKα1 were purchased from Fisher. siRNA oligonucleotides (20 nM) were transfected into cells using Lipofectamine RNAiMAX reagent (Invitrogen). After 12 h of transfection (transfection when cells were released from the second thymidine block) or after 48 h of transfection (transfection in non-synchronized cells), immunoblots were carried out to examine the knockdown of targeted proteins.

RNA isolation, reverse transcription, and quantitative PCR

Total RNA was isolated using an RNA extraction kit (Zymo Research, Irvine, CA) and was reverse-transcribed using random hexamer and Moloney murine leukemia virus reverse transcriptase (Invitrogen). SYBR Green-based quantitative RT-PCR for specific genes was performed using the Applied Biosystems real-time PCR system. Samples for each experimental condition were run in triplicate and were normalized to β_2 -microglobulin to determine relative expression levels. Primer sequences (Table S2) were obtained from the Primer Bank (113).

Protein extraction and Western blot analysis

Cells were harvested, lysed, and sonicated at 4 °C in a lysis buffer (50 mM Tris-HCl, pH 7.4, 150 mM NaCl, 0.5% SDS, 5 mM sodium pyrophosphate, protease, and phosphatase inhibitor tablet). Cell lysates were centrifuged at 13,000 $\times g$ for 15 min, and the supernatant was recovered. The protein concentrations were determined using the PierceTM BCA protein assay kit (Thermo Fisher Scientific). After 5 min boiling in 4 \times NuPAGE[®] LDS sample buffer with 10 \times reducing solution (Thermo Fisher Scientific), the proteins were separated by NuPAGE 4–12% protein gels (Thermo Fisher Scientific), transferred to polyvinylidene difluoride membranes by using the iBlot gel transfer device (Thermo Fisher Scientific), and probed with the appropriate primary antibodies (Table S1). Membrane-bound primary antibodies were detected using secondary antibodies conjugated with horseradish peroxidase. Immunoblots were developed on films using the enhanced chemiluminescence technique. Density of each band was analyzed by ImageJ software, and all values were normalized with actin. All image data are representative of at least two independent experiments.

Synchronization and cell-cycle analysis

HeLa cells were synchronized to the G₁/S border by double thymidine blockage and released into fresh medium for 7 h until they reached G₂ phase. In some experiments, HeLa cells were synchronized in mitosis by a shake-off after 14 h of incubation in 100 ng/ml nocodazole, washed, and allowed to transition to G₁ phase. U2OS cells were synchronized to M phase by 14 h of incubation in 100 ng/ml nocodazole.

BrdU incorporation was used to evaluate the amount of S-phase cells. In short, after labeling of cells with BrdU (Sigma-Aldrich), cells were fixed in ice-cold ethanol, treated with HCl to denature the DNA, and stained with PI and anti-BrdU antibody. Mitotic cells were examined by intracellular staining of phosphohistone H3 using a hypotonic buffer protocol described previously (114). Cell-cycle analysis was done with a flow cytometer (NovoCyte, ACEA Biosciences, San Diego, CA), and FlowJo version 10 was used to analyze the flow cytometry data.

In vitro phosphorylation

The bacterial expression vectors for GST-tagged CDC25 fragments were generated by PCR amplification of the encoding human CDC25C cDNA, followed by subcloning of the cDNA into pGEX-4T3 vector. Activated recombinant ERK (p42 MAPK) was prepared by incubating MBP-MAPK with constitutively activated MBP-MKK1 (115). GST- and MBP-

tagged recombinant proteins were expressed in bacteria and purified as described previously (49, 115, 116). AMP kinase was purchased from Millipore (Burlington, MA). The kinase reactions were performed in 10 μ l of reaction mixture (1 μ l of 10 \times kinase buffer and 0.25 mM ATP), AMPK (1 unit), and 1 μ g of the indicated substrates for 30 min at 30 °C. The reaction mixtures were boiled in SDS sample buffer and subjected to SDS-PAGE analysis and a Western blot assay.

Metabolic activity analysis

The radioactive tracers are described in Table S3. The activity of various metabolic pathways was determined by the rate of detritiation or ¹⁴CO₂ released from radioactive tracers, as described previously (117, 118). Specifically, glycolysis and fatty acid β -oxidation were determined by measuring the detritiation of [5-³H]glucose (119, 120) or by measuring the detritiation of [9,10-³H]palmitic acid (121), respectively. In brief, 1 million cells were suspended in 0.5 ml of fresh medium. The experiment was initiated by adding 1 μ Ci of radioactive tracer, and 2 h later, medium was transferred to a 1.5-ml microcentrifuge tube containing 50 μ l of 5 N HCl. The microcentrifuge tubes were then placed in 20-ml scintillation vials containing 0.5 ml of water with the vials capped and sealed. ³H₂O was separated from other radiolabeled metabolites by evaporation diffusion for 24 h at room temperature. A cell-free sample containing 1 μ Ci of radioactive tracer was included as a background control.

Glutaminolysis, TCA cycle (oxidation of pyruvate), and glucose oxidation flux through the PPP were determined by the rate of ¹⁴CO₂ released from [U-¹⁴C]glutamine (122), the rate of ¹⁴CO₂ released from [2-¹⁴C]pyruvate (123), and the rate of ¹⁴CO₂ released from [1-¹⁴C]glucose with some modifications (123). Whereas the difference in the rate of ¹⁴CO₂ released from [1-¹⁴C]glucose and [6-¹⁴C]glucose was used to determine the PPP activity, we consistently found that the ¹⁴CO₂ production from [6-¹⁴C]glucose was close to the background in cells. PPP activity was therefore determined as the rate of ¹⁴CO₂ released from [1-¹⁴C]glucose. In brief, 3 million cells were suspended in 0.5 ml of fresh medium. To facilitate the collection of ¹⁴CO₂, cells were dispensed into 7-ml glass vials (TS-13028, Thermo Fisher Scientific) with a PCR tube containing 50 μ l of 0.2 M KOH glued on the sidewall. After adding 0.5 μ Ci of radioactive tracer, the vials were capped using a screw cap with a rubber septum (TS-12713, Thermo Fisher Scientific). The assay was stopped 2 h later by injection of 100 μ l of 5 N HCl, and the vials were kept at room temperature overnight to trap the ¹⁴CO₂. The 50 μ l of KOH in the PCR tube was then transferred to scintillation vials containing 10 ml of scintillation solution for counting. A cell-free sample containing 0.5 μ Ci of radioactive tracer was included as a background control.

Phosphorylation of CDC25C in cells

HeLa cells were seeded at 4 $\times 10^5$ cells/35-mm dish and were transfected with 1.25 μ g of WT- or AS-AMPK α 2 and 1.25 μ g of WT- or S216A-Myc-CDC25C using the Lipofectamine (Thermo Fisher Scientific). Forty-eight hours after transfection, cells were washed twice with serum-free DMEM and incubated for 2 h before stimulation with 300 μ M A769662 for 20 min. Following stimulation,

AMPK phosphorylates CDC25C and regulates mitosis entry

200 μ l of phosphorylation buffer (20 mM HEPES (pH 7.3), 100 mM KOAc, 5 mM NaOAc, 2 mM MgOAc₂, 1 mM EGTA, 10 mM MgCl₂, 0.5 mM DTT, 5 mM creatine phosphate, 57 μ g/ml creatine kinase, 30 μ g/ml digitonin, 5 mM GTP (Abcam), 0.1 mM ATP, 0.1 mM N⁶-(phenethyl) ATP γ S (Abcam), 0.45 mM AMP (Abcam), 1 \times phosphatase inhibitor mixture I and II (Sigma), and 1 \times complete protease inhibitors (Sigma)) was added. After a 20-min incubation at room temperature, 200 μ l of 2 \times radio-immune precipitation assay buffer (100 mM Tris, pH 8, 300 mM NaCl, 2% Nonidet P-40, 0.2% SDS, and 20 mM EDTA) with 2.5 mM *p*-nitrobenzyl mesylate (Abcam) and 5% DMSO was added, and cells were incubated for an additional 1 h at room temperature. The cell lysates were then subjected to immunoprecipitation using agarose beads coupled to Myc tag antibody.

Constructs and generation of CDC25C-inducible stable cell lines

Plasmid pECE-AMPK α 2 WT, M93G, and pEBG-AMPK α 1 (1–312) were obtained from Addgene (Cambridge, MA) (82, 86). The pRetro-TRE3G vector (Clontech, Mountain View, CA) that expresses doxycycline-inducible CDC25C-S216A was generated by a recombination-based cloning method (In-Fusion Cloning Kits, Clontech) followed by site-directed mutagenesis (New England Biolabs, Ipswich, MA). Myc-tagged CDC25C-S216A expression plasmid was generated by subcloning pRetro-TRE3G-CDC25C-S216A into pCS2+MT plasmid.

The Amphopack 293 cells were transfected with the pRetro-TRE3G vector using Lipofectamine (Thermo Fisher Scientific) to produce retrovirus. HeLa cells that stably expressed reverse tetracycline-controlled transactivator (rtTA, Clontech) were infected with the retrovirus and treated with 2 μ g/ml puromycin (Sigma) and maintained in puromycin-containing medium.

Cell growth and cell death

Cell proliferations were measured by the IncuCyte cell proliferation assay. Cells were harvested by trypsinization, counted on a Countess automated cell counter (Invitrogen), and plated at 4000 cells/well on 96-well tissue culture plates in four replicates. Photomicrographs were taken every 3 h using an IncuCyte live cell imager (Essen Biosciences, Ann Arbor, MI), and confluence of the cultures was measured using IncuCyte software (Essen Biosciences) over 48 h in culture. For the cell death assay, cells were stained with annexin V–APC and PI and evaluated for apoptosis by flow cytometry according to the manufacturer's protocol (BD PharMingen, San Diego, CA).

Statistical analysis

p values were calculated with Student's *t* test. *p* values < 0.05 were considered significant, with *p* values < 0.05 and *p* values < 0.01 indicated as with single and double asterisks, respectively.

Author contributions—Y. S. data curation; Y. S. formal analysis; Y. S. validation; Y. S. and J. W. S. investigation; Y. S., J. W. S., and X. C. methodology; Y. S. and R. W. writing-original draft; Y. S., J. W. S., X. C., and R. W. writing-review and editing; R. W. conceptualization; R. W. supervision.

References

1. Robbins, E., and Morrill, G. A. (1969) Oxygen uptake during the HeLa cell life cycle and its correlation with macromolecular synthesis. *J. Cell Biol.* **43**, 629–633 [CrossRef Medline](#)
2. Bendick, C., Rasokat, H., and Steigleder, G. K. (1989) Azidothymidine-induced hyperpigmentation of skin and nails. *Arch. Dermatol.* **125**, 1285–1286 [CrossRef Medline](#)
3. Buchakjian, M. R., and Kornbluth, S. (2010) The engine driving the ship: metabolic steering of cell proliferation and death. *Nat. Rev. Mol. Cell Biol.* **11**, 715–727 [CrossRef Medline](#)
4. Cai, L., and Tu, B. P. (2012) Driving the cell cycle through metabolism. *Annu. Rev. Cell Dev. Biol.* **28**, 59–87 [CrossRef Medline](#)
5. Jorgensen, P., and Tyers, M. (2004) How cells coordinate growth and division. *Curr. Biol.* **14**, R1014–1027 [CrossRef Medline](#)
6. Lee, I. H., and Finkel, T. (2013) Metabolic regulation of the cell cycle. *Curr. Opin. Cell Biol.* **25**, 724–729 [CrossRef Medline](#)
7. Foster, D. A., Yellen, P., Xu, L., and Saqena, M. (2010) Regulation of G₁ cell cycle progression: distinguishing the restriction point from a nutrient-sensing cell growth checkpoint(s). *Genes Cancer* **1**, 1124–1131 [CrossRef Medline](#)
8. Hartwell, L. H., Culotti, J., Pringle, J. R., and Reid, B. J. (1974) Genetic control of the cell division cycle in yeast. *Science* **183**, 46–51 [CrossRef Medline](#)
9. Ho, A., and Dowdy, S. F. (2002) Regulation of G₁ cell-cycle progression by oncogenes and tumor suppressor genes. *Curr. Opin. Genet. Dev.* **12**, 47–52 [CrossRef Medline](#)
10. Pardee, A. B. (1974) A restriction point for control of normal animal cell proliferation. *Proc. Natl. Acad. Sci. U.S.A.* **71**, 1286–1290 [CrossRef Medline](#)
11. Sherr, C. J. (1996) Cancer cell cycles. *Science* **274**, 1672–1677 [CrossRef Medline](#)
12. Almeida, A., Bolaños, J. P., and Moncada, S. (2010) E3 ubiquitin ligase APC/C-Cdh1 accounts for the Warburg effect by linking glycolysis to cell proliferation. *Proc. Natl. Acad. Sci. U.S.A.* **107**, 738–741 [CrossRef Medline](#)
13. Birsoy, K., Wang, T., Chen, W. W., Freinkman, E., Abu-Remaileh, M., and Sabatini, D. M. (2015) An essential role of the mitochondrial electron transport chain in cell proliferation is to enable aspartate synthesis. *Cell* **162**, 540–551 [CrossRef Medline](#)
14. Colombo, S. L., Palacios-Callender, M., Frakich, N., De Leon, J., Schmitt, C. A., Boorn, L., Davis, N., and Moncada, S. (2010) Anaphase-promoting complex/cyclosome-Cdh1 coordinates glycolysis and glutaminolysis with transition to S phase in human T lymphocytes. *Proc. Natl. Acad. Sci. U.S.A.* **107**, 18868–18873 [CrossRef Medline](#)
15. Sullivan, L. B., Gui, D. Y., Hosios, A. M., Bush, L. N., Freinkman, E., and Vander Heiden, M. G. (2015) Supporting aspartate biosynthesis is an essential function of respiration in proliferating cells. *Cell* **162**, 552–563 [CrossRef Medline](#)
16. Ferrell, J. E., Jr. (2013) Feedback loops and reciprocal regulation: recurring motifs in the systems biology of the cell cycle. *Curr. Opin. Cell Biol.* **25**, 676–686 [CrossRef Medline](#)
17. Mitchison, J. M. (1972) *The Biology of the Cell Cycle*, pp. 192–200, Cambridge University Press, Cambridge, UK
18. Pederson, T. (2003) Historical review: an energy reservoir for mitosis, and its productive wake. *Trends Biochem. Sci.* **28**, 125–129 [CrossRef Medline](#)
19. Swann, M. M. (1957) The control of cell division: a review. I. General mechanisms. *Cancer Res.* **17**, 727–757 [Medline](#)
20. Di Talia, S., Skotheim, J. M., Bean, J. M., Siggia, E. D., and Cross, F. R. (2007) The effects of molecular noise and size control on variability in the budding yeast cell cycle. *Nature* **448**, 947–951 [CrossRef Medline](#)
21. Ginzberg, M. B., Kafri, R., and Kirschner, M. (2015) Cell biology: on being the right (cell) size. *Science* **348**, 1245075 [CrossRef Medline](#)
22. Martin, S. G., and Berthelot-Grosjean, M. (2009) Polar gradients of the DYRK-family kinase Pom1 couple cell length with the cell cycle. *Nature* **459**, 852–856 [CrossRef Medline](#)

23. Moseley, J. B., Mayeux, A., Paoletti, A., and Nurse, P. (2009) A spatial gradient coordinates cell size and mitotic entry in fission yeast. *Nature* **459**, 857–860 [CrossRef Medline](#)
24. Tzur, A., Kafri, R., LeBleu, V. S., Lahav, G., and Kirschner, M. W. (2009) Cell growth and size homeostasis in proliferating animal cells. *Science* **325**, 167–171 [CrossRef Medline](#)
25. Hardie, D. G., Ross, F. A., and Hawley, S. A. (2012) AMPK: a nutrient and energy sensor that maintains energy homeostasis. *Nat. Rev. Mol. Cell Biol.* **13**, 251–262 [CrossRef Medline](#)
26. Herzig, S., and Shaw, R. J. (2018) AMPK: guardian of metabolism and mitochondrial homeostasis. *Nat. Rev. Mol. Cell Biol.* **19**, 121–135 [CrossRef Medline](#)
27. Igata, M., Motoshima, H., Tsuruzoe, K., Kojima, K., Matsumura, T., Kondo, T., Taguchi, T., Nakamaru, K., Yano, M., Kukidome, D., Matsumoto, K., Toyonaga, T., Asano, T., Nishikawa, T., and Araki, E. (2005) Adenosine monophosphate-activated protein kinase suppresses vascular smooth muscle cell proliferation through the inhibition of cell cycle progression. *Circ. Res.* **97**, 837–844 [CrossRef Medline](#)
28. Imamura, K., Ogura, T., Kishimoto, A., Kaminishi, M., and Esumi, H. (2001) Cell cycle regulation via p53 phosphorylation by a 5'-AMP activated protein kinase activator, 5-aminoimidazole-4-carboxamide-1- β -D-ribofuranoside, in a human hepatocellular carcinoma cell line. *Biochem. Biophys. Res. Commun.* **287**, 562–567 [CrossRef Medline](#)
29. Liang, J., Shao, S. H., Xu, Z. X., Hennessy, B., Ding, Z., Larrea, M., Kondo, S., Dumont, D. J., Gutterman, J. U., Walker, C. L., Slingerland, J. M., and Mills, G. B. (2007) The energy sensing LKB1-AMPK pathway regulates p27(kip1) phosphorylation mediating the decision to enter autophagy or apoptosis. *Nat. Cell Biol.* **9**, 218–224 [CrossRef Medline](#)
30. Rattan, R., Giri, S., Singh, A. K., and Singh, I. (2005) 5-Aminoimidazole-4-carboxamide-1- β -D-ribofuranoside inhibits cancer cell proliferation *in vitro* and *in vivo* via AMP-activated protein kinase. *J. Biol. Chem.* **280**, 39582–39593 [CrossRef Medline](#)
31. Ben-Sahra, I., and Manning, B. D. (2017) mTORC1 signaling and the metabolic control of cell growth. *Curr. Opin. Cell Biol.* **45**, 72–82 [CrossRef Medline](#)
32. Fingar, D. C., Richardson, C. J., Tee, A. R., Cheatham, L., Tsou, C., and Blenis, J. (2004) mTOR controls cell cycle progression through its cell growth effectors S6K1 and 4E-BP1/eukaryotic translation initiation factor 4E. *Mol. Cell Biol.* **24**, 200–216 [CrossRef Medline](#)
33. Gwinn, D. M., Shackelford, D. B., Egan, D. F., Mihaylova, M. M., Mery, A., Vasquez, D. S., Turk, B. E., and Shaw, R. J. (2008) AMPK phosphorylation of raptor mediates a metabolic checkpoint. *Mol. Cell* **30**, 214–226 [CrossRef Medline](#)
34. Inoki, K., Zhu, T., and Guan, K. L. (2003) TSC2 mediates cellular energy response to control cell growth and survival. *Cell* **115**, 577–590 [CrossRef Medline](#)
35. Saxton, R. A., and Sabatini, D. M. (2017) mTOR signaling in growth, metabolism, and disease. *Cell* **169**, 361–371 [CrossRef Medline](#)
36. Shaw, R. J., Bardeesy, N., Manning, B. D., Lopez, L., Kosmatka, M., DePinho, R. A., and Cantley, L. C. (2004) The LKB1 tumor suppressor negatively regulates mTOR signaling. *Cancer Cell* **6**, 91–99 [CrossRef Medline](#)
37. Dunphy, W. G., Brizuela, L., Beach, D., and Newport, J. (1988) The *Xenopus* cdc2 protein is a component of MPF, a cytoplasmic regulator of mitosis. *Cell* **54**, 423–431 [CrossRef Medline](#)
38. Gautier, J., Norbury, C., Lohka, M., Nurse, P., and Maller, J. (1988) Purified maturation-promoting factor contains the product of a *Xenopus* homolog of the fission yeast cell cycle control gene *cdc2+*. *Cell* **54**, 433–439 [CrossRef Medline](#)
39. Morgan, D. O. (2006) *The Cell Cycle: Principles of Control*, 1st Ed., pp. 90–102, New Science Press, London, UK
40. Nurse, P. (1975) Genetic control of cell size at cell division in yeast. *Nature* **256**, 547–551 [CrossRef Medline](#)
41. King, R. W., Jackson, P. K., and Kirschner, M. W. (1994) Mitosis in transition. *Cell* **79**, 563–571 [CrossRef Medline](#)
42. Perdiguero, E., and Nebreda, A. R. (2004) Regulation of Cdc25C activity during the meiotic G₂/M transition. *Cell Cycle* **3**, 733–737 [Medline](#)
43. Crenshaw, D. G., Yang, J., Means, A. R., and Kornbluth, S. (1998) The mitotic peptidyl-prolyl isomerase, Pin1, interacts with Cdc25 and Plx1. *EMBO J.* **17**, 1315–1327 [CrossRef Medline](#)
44. Izumi, T., Walker, D. H., and Maller, J. L. (1992) Periodic changes in phosphorylation of the *Xenopus* cdc25 phosphatase regulate its activity. *Mol. Biol. Cell* **3**, 927–939 [CrossRef Medline](#)
45. Kumagai, A., and Dunphy, W. G. (1992) Regulation of the cdc25 protein during the cell cycle in *Xenopus* extracts. *Cell* **70**, 139–151 [CrossRef Medline](#)
46. Kumagai, A., and Dunphy, W. G. (1996) Purification and molecular cloning of Plx1, a Cdc25-regulatory kinase from *Xenopus* egg extracts. *Science* **273**, 1377–1380 [CrossRef Medline](#)
47. Perdiguero, E., Pillaire, M. J., Bodart, J. F., Hennersdorf, F., Frödin, M., Duesbery, N. S., Alonso, G., and Nebreda, A. R. (2003) Xp38 γ /SAPK3 promotes meiotic G₂/M transition in *Xenopus* oocytes and activates Cdc25C. *EMBO J.* **22**, 5746–5756 [CrossRef Medline](#)
48. Stukenberg, P. T., and Kirschner, M. W. (2001) Pin1 acts catalytically to promote a conformational change in Cdc25. *Mol. Cell* **7**, 1071–1083 [CrossRef Medline](#)
49. Wang, R., He, G., Nelman-Gonzalez, M., Ashorn, C. L., Gallick, G. E., Stukenberg, P. T., Kirschner, M. W., and Kuang, J. (2007) Regulation of Cdc25C by ERK-MAP kinases during the G₂/M transition. *Cell* **128**, 1119–1132 [CrossRef Medline](#)
50. Wang, R., Jung, S. Y., Wu, C. F., Qin, J., Kobayashi, R., Gallick, G. E., and Kuang, J. (2010) Direct roles of the signaling kinase RSK2 in Cdc25C activation during *Xenopus* oocyte maturation. *Proc. Natl. Acad. Sci. U.S.A.* **107**, 19885–19890 [CrossRef Medline](#)
51. Duckworth, B. C., Weaver, J. S., and Ruderman, J. V. (2002) G₂ arrest in *Xenopus* oocytes depends on phosphorylation of cdc25 by protein kinase A. *Proc. Natl. Acad. Sci. U.S.A.* **99**, 16794–16799 [CrossRef Medline](#)
52. Margolis, S. S., Perry, J. A., Forester, C. M., Nutt, L. K., Guo, Y., Jardim, M. J., Thomenius, M. J., Freel, C. D., Darbandi, R., Ahn, J. H., Arroyo, J. D., Wang, X. F., Shenolikar, S., Nairn, A. C., Dunphy, W. G., *et al.* (2006) Role for the PP2A/B56 δ phosphatase in regulating 14-3-3 release from Cdc25 to control mitosis. *Cell* **127**, 759–773 [CrossRef Medline](#)
53. Margolis, S. S., Walsh, S., Weiser, D. C., Yoshida, M., Shenolikar, S., and Kornbluth, S. (2003) PP1 control of M phase entry exerted through 14-3-3-regulated Cdc25 dephosphorylation. *EMBO J.* **22**, 5734–5745 [CrossRef Medline](#)
54. Sanchez, Y., Wong, C., Thoma, R. S., Richman, R., Wu, Z., Piwnicka-Worms, H., and Elledge, S. J. (1997) Conservation of the Chk1 checkpoint pathway in mammals: linkage of DNA damage to Cdk regulation through Cdc25. *Science* **277**, 1497–1501 [CrossRef Medline](#)
55. Takizawa, C. G., and Morgan, D. O. (2000) Control of mitosis by changes in the subcellular location of cyclin-B1-Cdk1 and Cdc25C. *Curr. Opin. Cell Biol.* **12**, 658–665 [CrossRef Medline](#)
56. Ferrell, J. E., Jr., and Ha, S. H. (2014) Ultrasensitivity part II: multisite phosphorylation, stoichiometric inhibitors, and positive feedback. *Trends Biochem. Sci.* **39**, 556–569 [CrossRef Medline](#)
57. Boutros, R., Lobjois, V., and Ducommun, B. (2007) CDC25 phosphatases in cancer cells: key players? Good targets? *Nat. Rev. Cancer* **7**, 495–507 [CrossRef Medline](#)
58. Donzelli, M., and Draetta, G. F. (2003) Regulating mammalian checkpoints through Cdc25 inactivation. *EMBO Rep.* **4**, 671–677 [CrossRef Medline](#)
59. Karlsson-Rosenthal, C., and Millar, J. B. (2006) Cdc25: mechanisms of checkpoint inhibition and recovery. *Trends Cell Biol.* **16**, 285–292 [CrossRef Medline](#)
60. Reinhardt, H. C., and Yaffe, M. B. (2009) Kinases that control the cell cycle in response to DNA damage: Chk1, Chk2, and MK2. *Curr. Opin. Cell Biol.* **21**, 245–255 [CrossRef Medline](#)
61. Furnari, B., Rhind, N., and Russell, P. (1997) Cdc25 mitotic inducer targeted by chk1 DNA damage checkpoint kinase. *Science* **277**, 1495–1497 [CrossRef Medline](#)
62. Peng, C. Y., Graves, P. R., Thoma, R. S., Wu, Z., Shaw, A. S., and Piwnicka-Worms, H. (1997) Mitotic and G₂ checkpoint control: regulation of 14-3-3 protein binding by phosphorylation of Cdc25C on serine-216. *Science* **277**, 1501–1505 [CrossRef Medline](#)

AMPK phosphorylates CDC25C and regulates mitosis entry

63. Corton, J. M., Gillespie, J. G., Hawley, S. A., and Hardie, D. G. (1995) 5-Aminoimidazole-4-carboxamide ribonucleoside: a specific method for activating AMP-activated protein kinase in intact cells? *Eur. J. Biochem.* **229**, 558–565 [CrossRef Medline](#)
64. Day, P., Sharff, A., Parra, L., Cleasby, A., Williams, M., Hörer, S., Nar, H., Redemann, N., Tickle, I., and Yon, J. (2007) Structure of a CBS-domain pair from the regulatory γ 1 subunit of human AMPK in complex with AMP and ZMP. *Acta Crystallogr. D Biol. Crystallogr.* **63**, 587–596 [CrossRef Medline](#)
65. Grahame Hardie, D. (2016) Regulation of AMP-activated protein kinase by natural and synthetic activators. *Acta Pharm. Sin. B* **6**, 1–19 [CrossRef Medline](#)
66. Sanders, M. J., Ali, Z. S., Hegarty, B. D., Heath, R., Snowden, M. A., and Carling, D. (2007) Defining the mechanism of activation of AMP-activated protein kinase by the small molecule A-769662, a member of the thienopyridone family. *J. Biol. Chem.* **282**, 32539–32548 [CrossRef Medline](#)
67. Foretz, M., Guigas, B., Bertrand, L., Pollak, M., and Viollet, B. (2014) Metformin: from mechanisms of action to therapies. *Cell Metab.* **20**, 953–966 [CrossRef Medline](#)
68. Branzei, D., and Foiani, M. (2008) Regulation of DNA repair throughout the cell cycle. *Nat. Rev. Mol. Cell Biol.* **9**, 297–308 [CrossRef Medline](#)
69. Hustedt, N., and Durocher, D. (2016) The control of DNA repair by the cell cycle. *Nat. Cell Biol.* **19**, 1–9 [Medline](#)
70. Langerak, P., and Russell, P. (2011) Regulatory networks integrating cell cycle control with DNA damage checkpoints and double-strand break repair. *Phil. Trans. R. Soc. Lond. B Biol. Sci.* **366**, 3562–3571 [CrossRef Medline](#)
71. Zhou, B. B., and Elledge, S. J. (2000) The DNA damage response: putting checkpoints in perspective. *Nature* **408**, 433–439 [CrossRef Medline](#)
72. Giglia-Mari, G., Zotter, A., and Vermeulen, W. (2011) DNA damage response. *Cold Spring Harb. Perspect. Biol.* **3**, a000745 [Medline](#)
73. Jones, R. G., Plas, D. R., Kubek, S., Buzzai, M., Mu, J., Xu, Y., Birnbaum, M. J., and Thompson, C. B. (2005) AMP-activated protein kinase induces a p53-dependent metabolic checkpoint. *Mol. Cell* **18**, 283–293 [CrossRef Medline](#)
74. Taylor, W. R., and Stark, G. R. (2001) Regulation of the G₂/M transition by p53. *Oncogene* **20**, 1803–1815 [CrossRef Medline](#)
75. Vousden, K. H., and Lu, X. (2002) Live or let die: the cell's response to p53. *Nat. Rev. Cancer* **2**, 594–604 [CrossRef Medline](#)
76. Hochegger, H., Takeda, S., and Hunt, T. (2008) Cyclin-dependent kinases and cell-cycle transitions: does one fit all? *Nat. Rev. Mol. Cell Biol.* **9**, 910–916 [CrossRef Medline](#)
77. Malumbres, M., and Barbacid, M. (2009) Cell cycle, CDKs and cancer: a changing paradigm. *Nat. Rev. Cancer* **9**, 153–166 [CrossRef Medline](#)
78. Matlashewski, G., Banks, L., Pim, D., and Crawford, L. (1986) Analysis of human p53 proteins and mRNA levels in normal and transformed cells. *Eur. J. Biochem.* **154**, 665–672 [CrossRef Medline](#)
79. May, E., Jenkins, J. R., and May, P. (1991) Endogenous HeLa p53 proteins are easily detected in HeLa cells transfected with mouse deletion mutant p53 gene. *Oncogene* **6**, 1363–1365 [Medline](#)
80. Scott, J. W., Norman, D. G., Hawley, S. A., Kontogiannis, L., and Hardie, D. G. (2002) Protein kinase substrate recognition studied using the recombinant catalytic domain of AMP-activated protein kinase and a model substrate. *J. Mol. Biol.* **317**, 309–323 [CrossRef Medline](#)
81. Yaffe, M. B., Leparo, G. G., Lai, J., Obata, T., Volinia, S., and Cantley, L. C. (2001) A motif-based profile scanning approach for genome-wide prediction of signaling pathways. *Nat. Biotechnol.* **19**, 348–353 [CrossRef Medline](#)
82. Egan, D. F., Shackelford, D. B., Mihaylova, M. M., Gelino, S., Kohnz, R. A., Mair, W., Vasquez, D. S., Joshi, A., Gwinn, D. M., Taylor, R., Asara, J. M., Fitzpatrick, J., Dillin, A., Viollet, B., Kundu, M., *et al.* (2011) Phosphorylation of ULK1 (hATG1) by AMP-activated protein kinase connects energy sensing to mitophagy. *Science* **331**, 456–461 [CrossRef Medline](#)
83. Alaimo, P. J., Shogren-Knaak, M. A., and Shokat, K. M. (2001) Chemical genetic approaches for the elucidation of signaling pathways. *Curr. Opin. Chem. Biol.* **5**, 360–367 [CrossRef Medline](#)
84. Allen, J. J., Lazerwith, S. E., and Shokat, K. M. (2005) Bio-orthogonal affinity purification of direct kinase substrates. *J. Am. Chem. Soc.* **127**, 5288–5289 [CrossRef Medline](#)
85. Allen, J. J., Li, M., Brinkworth, C. S., Paulson, J. L., Wang, D., Hübner, A., Chou, W. H., Davis, R. J., Burlingame, A. L., Messing, R. O., Katayama, C. D., Hedrick, S. M., and Shokat, K. M. (2007) A semisynthetic epitope for kinase substrates. *Nat. Methods* **4**, 511–516 [CrossRef Medline](#)
86. Banko, M. R., Allen, J. J., Schaffer, B. E., Wilker, E. W., Tsou, P., White, J. L., Villén, J., Wang, B., Kim, S. R., Sakamoto, K., Gygi, S. P., Cantley, L. C., Yaffe, M. B., Shokat, K. M., and Brunet, A. (2011) Chemical genetic screen for AMPK α 2 substrates uncovers a network of proteins involved in mitosis. *Mol. Cell* **44**, 878–892 [CrossRef Medline](#)
87. Boutros, R., Dozier, C., and Ducommun, B. (2006) The when and wheres of CDC25 phosphatases. *Curr. Opin. Cell Biol.* **18**, 185–191 [CrossRef Medline](#)
88. Perry, J. A., and Kornbluth, S. (2007) Cdc25 and Wee1: analogous opposites? *Cell Div.* **2**, 12 [CrossRef Medline](#)
89. Hirai, H., Iwasawa, Y., Okada, M., Arai, T., Nishibata, T., Kobayashi, M., Kimura, T., Kaneko, N., Ohtani, J., Yamanaka, K., Itadani, H., Takahashi-Suzuki, I., Fukasawa, K., Oki, H., Nambu, T., *et al.* (2009) Small-molecule inhibition of Wee1 kinase by MK-1775 selectively sensitizes p53-deficient tumor cells to DNA-damaging agents. *Mol. Cancer Ther.* **8**, 2992–3000 [CrossRef Medline](#)
90. McGowan, C. H., and Russell, P. (1995) Cell cycle regulation of human WEE1. *EMBO J.* **14**, 2166–2175 [Medline](#)
91. Wang, Y., Jacobs, C., Hook, K. E., Duan, H., Booher, R. N., and Sun, Y. (2000) Binding of 14-3-3 β to the carboxyl terminus of Wee1 increases Wee1 stability, kinase activity, and G₂-M cell population. *Cell Growth Differ.* **11**, 211–219 [Medline](#)
92. Watanabe, N., Broome, M., and Hunter, T. (1995) Regulation of the human WEE1Hu CDK tyrosine 15-kinase during the cell cycle. *EMBO J.* **14**, 1878–1891 [Medline](#)
93. Hardie, D. G., Schaffer, B. E., and Brunet, A. (2016) AMPK: an energy-sensing pathway with multiple inputs and outputs. *Trends Cell Biol.* **26**, 190–201 [CrossRef Medline](#)
94. Hurley, R. L., Anderson, K. A., Franzone, J. M., Kemp, B. E., Means, A. R., and Witters, L. A. (2005) The Ca²⁺/calmodulin-dependent protein kinase kinases are AMP-activated protein kinase kinases. *J. Biol. Chem.* **280**, 29060–29066 [CrossRef Medline](#)
95. Hardie, D. G., and Alessi, D. R. (2013) LKB1 and AMPK and the cancer-metabolism link: ten years after. *BMC Biol.* **11**, 36 [CrossRef Medline](#)
96. Shackelford, D. B., and Shaw, R. J. (2009) The LKB1-AMPK pathway: metabolism and growth control in tumour suppression. *Nat. Rev. Cancer* **9**, 563–575 [CrossRef Medline](#)
97. Hartwell, L. H., and Weinert, T. A. (1989) Checkpoints: controls that ensure the order of cell cycle events. *Science* **246**, 629–634 [CrossRef Medline](#)
98. Kastan, M. B., and Bartek, J. (2004) Cell-cycle checkpoints and cancer. *Nature* **432**, 316–323 [CrossRef Medline](#)
99. Weinert, T. A., and Hartwell, L. H. (1988) The RAD9 gene controls the cell cycle response to DNA damage in *Saccharomyces cerevisiae*. *Science* **241**, 317–322 [CrossRef Medline](#)
100. Hand, S. C., and Hardewig, I. (1996) Downregulation of cellular metabolism during environmental stress: mechanisms and implications. *Annu. Rev. Physiol.* **58**, 539–563 [CrossRef Medline](#)
101. Kültz, D. (2003) Evolution of the cellular stress proteome: from monophyletic origin to ubiquitous function. *J. Exp. Biol.* **206**, 3119–3124 [CrossRef Medline](#)
102. Wang, R., and Green, D. R. (2012) Metabolic checkpoints in activated T cells. *Nat. Immunol.* **13**, 907–915 [CrossRef Medline](#)
103. Kültz, D. (2005) Molecular and evolutionary basis of the cellular stress response. *Annu. Rev. Physiol.* **67**, 225–257 [CrossRef Medline](#)
104. Hochachka, P. W., and Somero, G. N. (2002) *Biochemical Adaptation: Mechanism and Process in Physiological Evolution*, 3rd Ed., pp. 101–157, Oxford University Press, Oxford, UK
105. Green, D. R., and Fitzgerald, P. (2016) Just so stories about the evolution of apoptosis. *Curr. Biol.* **26**, R620–R627 [CrossRef Medline](#)
106. Kawabe, T. (2004) G₂ checkpoint abrogators as anticancer drugs. *Mol. Cancer Ther.* **3**, 513–519 [Medline](#)

107. Shapiro, G. I., and Harper, J. W. (1999) Anticancer drug targets: cell cycle and checkpoint control. *J. Clin. Invest.* **104**, 1645–1653 [CrossRef Medline](#)
108. Do, K., Wilsker, D., Ji, J., Zlott, J., Freshwater, T., Kinders, R. J., Collins, J., Chen, A. P., Doroshow, J. H., and Kummar, S. (2015) Phase I study of single-agent AZD1775 (MK-1775), a Wee1 kinase inhibitor, in patients with refractory solid tumors. *J. Clin. Oncol.* **33**, 3409–3415 [CrossRef Medline](#)
109. Leijen, S., van Geel, R. M., Pavlick, A. C., Tibes, R., Rosen, L., Razak, A. R., Lam, R., Demuth, T., Rose, S., Lee, M. A., Freshwater, T., Shumway, S., Liang, L. W., Oza, A. M., Schellens, J. H., and Shapiro, G. I. (2016) Phase I study evaluating WEE1 inhibitor AZD1775 as monotherapy and in combination with gemcitabine, cisplatin, or carboplatin in patients with advanced solid tumors. *J. Clin. Oncol.* **34**, 4371–4380 [CrossRef Medline](#)
110. Aarts, M., Sharpe, R., Garcia-Murillas, I., Gevensleben, H., Hurd, M. S., Shumway, S. D., Toniatti, C., Ashworth, A., and Turner, N. C. (2012) Forced mitotic entry of S-phase cells as a therapeutic strategy induced by inhibition of WEE1. *Cancer Disc.* **2**, 524–539 [CrossRef Medline](#)
111. Mir, S. E., De Witt Hamer, P. C., Krawczyk, P. M., Balaj, L., Claes, A., Niers, J. M., Van Tilborg, A. A., Zwinderman, A. H., Geerts, D., Kaspers, G. J., Peter Vandertop, W., Cloos, J., Tannous, B. A., Wesseling, P., Aten, J. A., et al. (2010) *In silico* analysis of kinase expression identifies WEE1 as a gatekeeper against mitotic catastrophe in glioblastoma. *Cancer Cell* **18**, 244–257 [CrossRef Medline](#)
112. Mueller, S., and Haas-Kogan, D. A. (2015) WEE1 kinase as a target for cancer therapy. *J. Clin. Oncol.* **33**, 3485–3487 [CrossRef Medline](#)
113. Wang, X., Spandidos, A., Wang, H., and Seed, B. (2012) PrimerBank: a PCR primer database for quantitative gene expression analysis, 2012 update. *Nucleic Acids Res.* **40**, D1144–D1149 [CrossRef Medline](#)
114. Shen, Y., Vignali, P., and Wang, R. (2017) Rapid profiling cell cycle by flow cytometry using concurrent staining of DNA and mitotic markers. *Bio Protoc.* **7**, e2517 [CrossRef Medline](#)
115. Rouse, J., Cohen, P., Trigon, S., Morange, M., Alonso-Llamazares, A., Zamanillo, D., Hunt, T., and Nebreda, A. R. (1994) A novel kinase cascade triggered by stress and heat shock that stimulates MAPKAP kinase-2 and phosphorylation of the small heat shock proteins. *Cell* **78**, 1027–1037 [CrossRef Medline](#)
116. Palmer, A., Gavin, A. C., and Nebreda, A. R. (1998) A link between MAP kinase and p34(cdc2)/cyclin B during oocyte maturation: p90(rsk) phosphorylates and inactivates the p34(cdc2) inhibitory kinase Myt1. *EMBO J.* **17**, 5037–5047 [CrossRef Medline](#)
117. Liu, L., Lu, Y., Martinez, J., Bi, Y., Lian, G., Wang, T., Milasta, S., Wang, J., Yang, M., Liu, G., Green, D. R., and Wang, R. (2016) Proinflammatory signal suppresses proliferation and shifts macrophage metabolism from Myc-dependent to HIF1 α -dependent. *Proc. Natl. Acad. Sci. U.S.A.* **113**, 1564–1569 [CrossRef Medline](#)
118. Wang, R., Dillon, C. P., Shi, L. Z., Milasta, S., Carter, R., Finkelstein, D., McCormick, L. L., Fitzgerald, P., Chi, H., Munger, J., and Green, D. R. (2011) The transcription factor Myc controls metabolic reprogramming upon T lymphocyte activation. *Immunity* **35**, 871–882 [CrossRef Medline](#)
119. Goodwin, G. W., Cohen, D. M., and Taegtmeier, H. (2001) [3 H]Glucose overestimates glycolytic flux in isolated working rat heart: role of the pentose phosphate pathway. *Am. J. Physiol. Endocrinol. Metab.* **280**, E502–E508 [CrossRef Medline](#)
120. Neely, J. R., Denton, R. M., England, P. J., and Randle, P. J. (1972) The effects of increased heart work on the tricarboxylate cycle and its interactions with glycolysis in the perfused rat heart. *Biochem. J.* **128**, 147–159 [CrossRef Medline](#)
121. Moon, A., and Rhead, W. J. (1987) Complementation analysis of fatty acid oxidation disorders. *J. Clin. Invest.* **79**, 59–64 [CrossRef Medline](#)
122. Brand, K., Williams, J. F., and Weidemann, M. J. (1984) Glucose and glutamine metabolism in rat thymocytes. *Biochem. J.* **221**, 471–475 [CrossRef Medline](#)
123. Willems, H. L., de Kort, T. F., Trijbels, F. J., Monnens, L. A., and Veerkamp, J. H. (1978) Determination of pyruvate oxidation rate and citric acid cycle activity in intact human leukocytes and fibroblasts. *Clin. Chem.* **24**, 200–203 [Medline](#)